

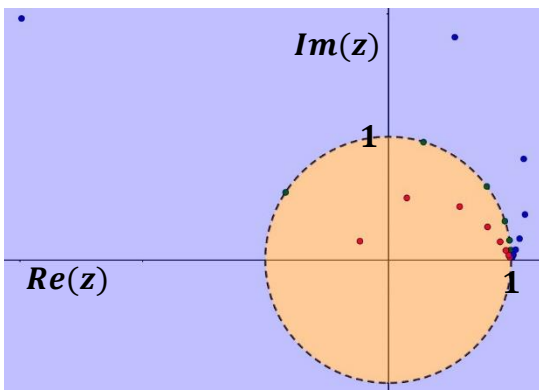
Julia sets and the Mandelbrot set

To understand the logistic map $x \rightarrow rx(1 - x)$ or its equivalent $x \rightarrow x^2 + a$ in full requires the use of complex numbers, just as the understanding of roots for real polynomials $\sum a_k x^k = 0$ with $a_k \in \mathbb{R}$ becomes so much clearer when the question is widened to the question of roots for complex polynomials $\sum c_k z^k = 0$ with $c_k \in \mathbb{C}$.

The iteration $z_{k+1} = z_k^2 + c$ with a constant $c \in \mathbb{C}$ seems innocent, the simplest of all non-linear iterations but in it lies the root of much beauty and complexity. It contains all the basic elements that you can expect to find in every non-linear iteration.

Fixpoints, Cycles and Basins of attractions

Finding fixpoints of the iteration $f_c(z) = z^2 + c$ and $c = 0$ leads to $z = z^2$ with two solutions $z = 0$ and $z = 1$. For a general point $z = re^{i\varphi}$ the iteration breaks down to $r \rightarrow r^2$ and $\varphi \rightarrow 2\varphi \pmod{2\pi}$ (stretch and 'fold').



Picture of z_0, \dots, z_6 for three different initial values close to $z_0 = 1$.

$|z_0| < 1$ leads to ingoing spirals.

$|z_0| = 1$ leads to iterates that stay on the unit circle.

$|z_0| > 1$ leads to outgoing spirals.

$z_0 = 0$ is an **attracting fixpoint**. All points with $|z| < 1$ iterate towards $z_0 = 0$. $|z| < 1$ is the **basin of attraction**, $A(z_0)$.

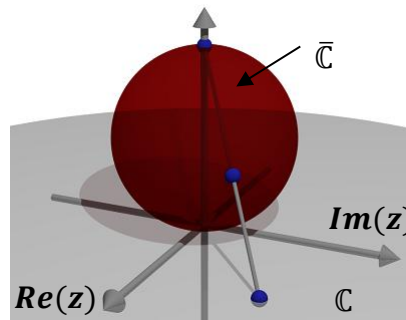
The unit circle contains cycles of any length. $z_0 = e^{i \cdot 2\pi/n}$ gives a cycle forming a regular n -gon. $z_0 = e^{i\varphi_0}$ with $\varphi_0 \in \mathbb{R} \setminus \mathbb{Q}$ gives an infinite and irregular sequence of iterates.

Fixpoints with $f(z_0) = z_0$ and **cycles** $z_0 \rightarrow \dots \rightarrow z_{n-1} \rightarrow z_0$ of period n with $f^n(z_0) = z_0$ are classified as:

- | | | |
|-----------------------------------|---------------------|-------------------------|
| 1. Superattracting: | $f'(z_0) = 0$ | $D(f^n(z_0)) = 0$ |
| 2. Attracting: | $0 < f'(z_0) < 1$ | $0 < D(f^n(z_0)) < 1$ |
| 3. Neutral or Indifferent: | $ f'(z_0) = 1$ | $ D(f^n(z_0)) = 1$ |
| 4. Repelling: | $ f'(z_0) > 1$ | $ D(f^n(z_0)) > 1$ |

If the complex plane is expanded with a point at infinity $\bar{\mathbb{C}} = \mathbb{C} \cup \{\infty\}$ we get the Riemann sphere, often illustrated with a stereographic projection.

In $\bar{\mathbb{C}}$ there is a new attractive fixpoint at $z = \infty$, with $|z| > 1$ as basin of attraction.



Every point on the sphere $\bar{\mathbb{C}}$ except the north pole projects to a point in \mathbb{C} . The south pole projects to $(0,0)$ and the north pole project to an imaginary point at infinity.

The Riemann sphere is a compact version of the complex plane. The dynamics of f_c around $z = \infty$ can be studied at $z = 0$ via a change of coordinates $h(z) = 1/z$ which takes ∞ to 0 and transforms f_c into g_c where $g_c(z) = z^2/(1 + cz^2)$ and $g'_c(0) = 0$. In this light ∞ is a superattracting fixpoint of $f_c(\infty)$.

The complex plane of initial values z_0 is divided into two subsets, one called the **escape set** E consists of points z_0 for which the iterates escapes, $\lim_{k \rightarrow \infty} z_k = \infty$. The escapes set is the basin of attraction of the point at infinity.

The complement of the escape set is the **prisoner set** P , consisting of points where the iterates remain bounded.

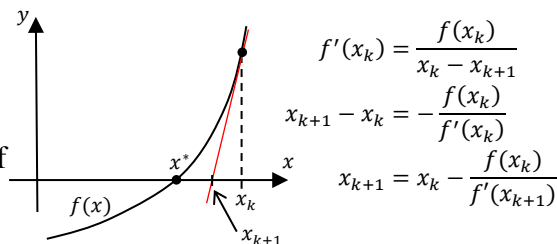
Escape sets: $E_c \equiv \{z_0 \mid \lim_{k \rightarrow \infty} z_k = \infty \text{ where } z_{k+1} = z_k^2 + c\}$ E_0 is $|z| > 1$

Prisoner sets: $P_c = \{z_0 \mid z_0 \notin E_c\}$ P_0 is $|z| \leq 1$

The boundary between the prisoner set P_c and the escape set E_c is called the **Julia set**, $J_c \equiv \partial E_c = \partial P_c$.

J_0 is the unit circle, it contains both a repelling fixpoint, cycles of arbitrary length and chaotic sequences of iterates. Other values of c leads to other Julia sets.

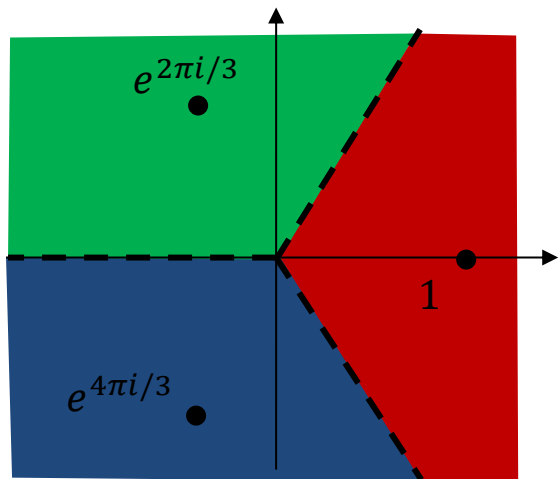
The historical roots and a nice illustration of ‘basins of attraction’ in the complex plane comes from Newton’s method for finding approximations of roots to an equation $f(x) = 0$ by a sequence of iterations approaching a value x^* for which $f(x^*) = 0$.



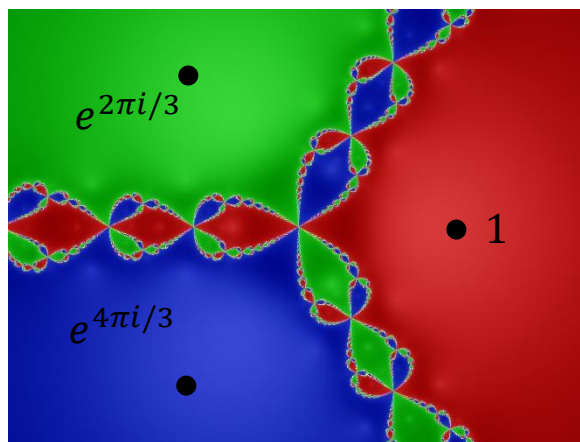
Newton’s method to $z^3 = 1$ which has $f(z) = z^3 - 1$ and three roots $z_k = e^{i \cdot k \cdot \frac{2\pi}{3}}$ with $k = 0, 1, 2$ gives:

$$z_{k+1} = z_k - \frac{z_k^3 - 1}{3z_k^2}$$

The three roots are like magnets to the iteration. Which initial value z_0 will end up at which root or in other words, what are the basins of attraction of the attracting fixpoints z_0, z_1 and z_2 ?



Wrong



Right

In the correct picture the three basins of attraction have a common boundary, not what you normally get when you divide an area into three pieces. The boundary is another example of a Julia set. Every neighbourhood of every point contain all three colours and points on the boundary iterates to other points on the boundary.

The behaviour of iterations is regular on the inner parts of the prisoner and escape sets. Only on the Julia set do we see chaotic behaviour. Before delving deeper into the properties of Julia sets, a definition of **chaotic system**.

A function $f: \Lambda \rightarrow \Lambda$ is **chaotic** if f it has **sensitive dependence on initial conditions (SDIC)** which means that points arbitrarily closed separates at an exponential rate with a given metric $d(x, y)$.

For any $x \in \Lambda$ and any $\delta > 0$ there is a y with $0 < d(x, y) < \delta$ s.t. $d(f^n(x), f^n(y)) > e^{an}d(x, y)$ for some a .

The opposite is to be **stable**, no point has a neighbourhood with points that depart exponentially. We assume a bounded metric for \bar{C} so that orbits that are attracted to ∞ can still have distances tending to zero which makes E_c a stable region. To get an easier criterion for chaos we need the topological notion of transitivity.

Transitivity:

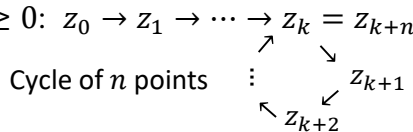
A continuous f is transitive on X if for every pair of open sets $A, B \subset X$, there is $n > 0$ s.t. $f^n(A) \cap B \neq \emptyset$. This means that f mixes the content of A into every open subset.

The following theorem gives an easier criterion for chaos of $f: \Lambda \rightarrow \Lambda$ on an infinite set Λ :

$\left\{ \begin{array}{l} \text{Periodic points of } f \text{ are dense in } \Lambda \\ f \text{ is transitive on } \Lambda \end{array} \right. \Rightarrow f \text{ is chaotic on } \Lambda.$

Notations and definitions:

- Fixed point** Point such that $f(z_0) = z_0$
- Periodic point** Point for which $f^n(z_0) = z_0$ and where the least such n is the **period** and $n > 1$.
- Critical point** Point where $f'(z_0) = 0$
- Orbit of z_0 under f** The sequence $z_0, z_1, z_2, \dots = \mathcal{O}_f(z_0)$, a.k.a **forward orbit** $\mathcal{O}_f^+(z_0)$
- Preperiodic point** $f^{k+n}(z_0) = f^k(z_0)$ for some $k > 0$ and $n \geq 0$: $z_0 \rightarrow z_1 \rightarrow \dots \rightarrow z_k = z_{k+n}$
- Critical orbit** Orbit of critical point



Julia sets

Definition:

The **Julia set** of $f(z)$ denoted by $J(f)$ is the set of all points at which f has SDIC, or in other words: $J(f)$ is the chaotic set of f . The complement of $J(f)$ is the **Fatou set** $F(f)$ which is the stable set of f .

Alternative characterizations of Julia sets:

J_c is the closure of the set of repelling periodic points of f_c . For $c = 0$ they are $e^{2\pi i \cdot p/q}$ with $p \neq 0$

J_c is the boundary of P_c and E_c , $J_c = \partial P_c$.

$J_c = \partial E_c$ (This holds only when ∞ is superattracting, as it is for polynomials).

Julia sets and Fatou sets can be defined for every non-constant holomorphic function f from $\bar{\mathbb{C}}$ onto $\bar{\mathbb{C}}$ which are the same as the rational functions $f(z) = p(z)/q(z)$. Holomorphic means complex differentiable in a neighbourhood of every point in its domain.

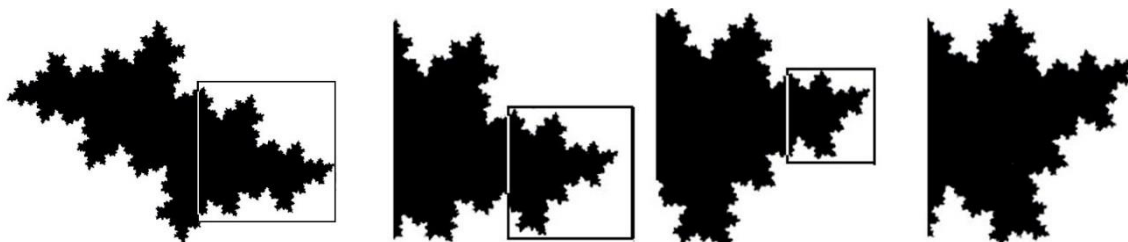
For such f there are a finite number of open sets F_1, \dots, F_r . These sets are called Fatou domains of $f(z)$. Their union is the Fatou set $F(f) = F_1 \cup \dots \cup F_r$. The Fatou set is dense in \mathbb{C} . Each Fatou domain contains at least one critical point where $f'(z) = 0$ or $f(z) = \infty$.

Newton's method on $z^3 = 1$ lead to $f(z) = z - (z^3 - 1)/3z^2$ where F_k are the attracting regions of the roots. Red, green and blue parts in the image

The complement of the Fatou set is the Julia set $J(f) = F(f)^c$. If $J(f) \neq \bar{\mathbb{C}}$ then it is nowhere dense (without interior points) and uncountable. Only a countable number of points in $J(f)$ have finite iterations and points outside this set behaves chaotically as we have seen in the example with $z \rightarrow z^2$ on the unit circle.

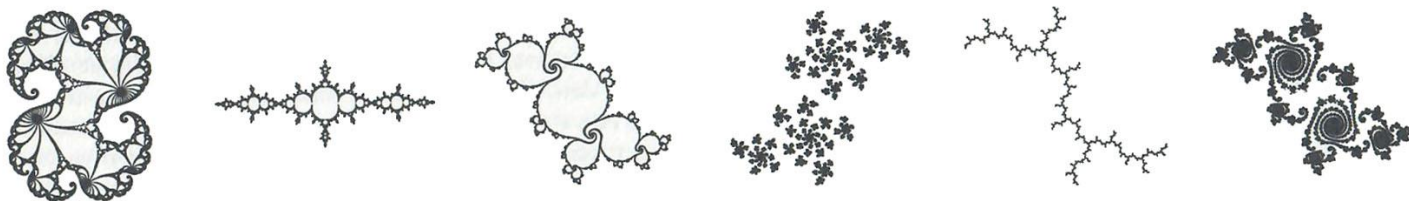
$f_c(z) = z^2 + c$ covers the general case of quadratic maps $q(z) = \alpha z^2 + \beta z + \gamma$ since $H(z) = \alpha z + \beta/2$ gives a conjugation between q and f_c . $H \circ q = f_c \circ H$ leads to $H \circ q^n = f_c^n \circ H$ which means a one-to-one correspondence between orbits of f_c and orbits of q , they are dynamically equivalent. Focus will be on f_c .

The Julia set of $f_c(z) = z^2 + c$ is denoted J_c . J_0 is the boundary of the unit disc $\mathbb{D} \equiv \{z: |z| < 1\}$, $J_0 = \partial \mathbb{D}$.



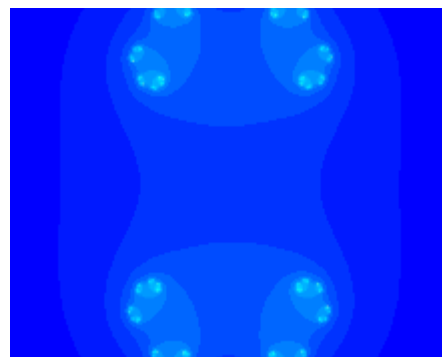
The black part is the interior of J_c at $c = -0.5 + 0.5i$. Note the self-similarity at different scales.

Most Julia sets have an intricate structure with fractal geometry and self-similarity.



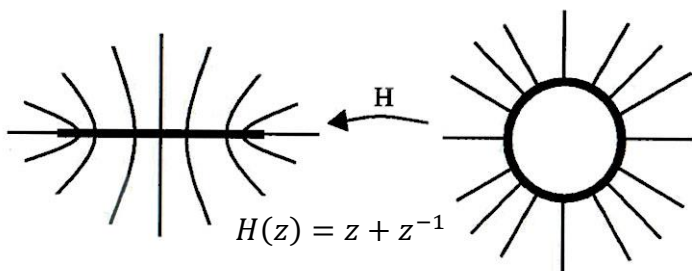
Julia sets come in different forms, some are connected, some pinched together at certain points, others are like an archipelago of disconnected islands, some are like tendrils, others like fireworks and flames with tails like seahorses. The looks of Julia sets can be explored in MANDELBRROT on the top menu where the interior of J_c is shown in one colour and points outside are coloured based on proximity.

Animation of Julia set for $z^2 + 0.7885e^{i\varphi}$ with $\varphi \in [0, 2\pi]$



The illustration of Julia sets in the animation and the MANDRELBROT program are based on an algorithm that starts from a grid of points in \mathbb{C} and computes $f_c^k(z)$ for each of them up to $k \leq N$ for some chosen N . If $|f_c^k(z)|$ exceeds some given limit for a certain k then $z \in E_c$ and k decides the color of the point. If $f_c^k(z)$ never exceeds the outer limit it is assumed that z is part of the prisoner set P_c and gets a certain color.

The only two Julia sets in the family J_c that are not fractal are $J_0 = \partial\mathbb{D}$ and $J_{-2} = [-2, 2]$.

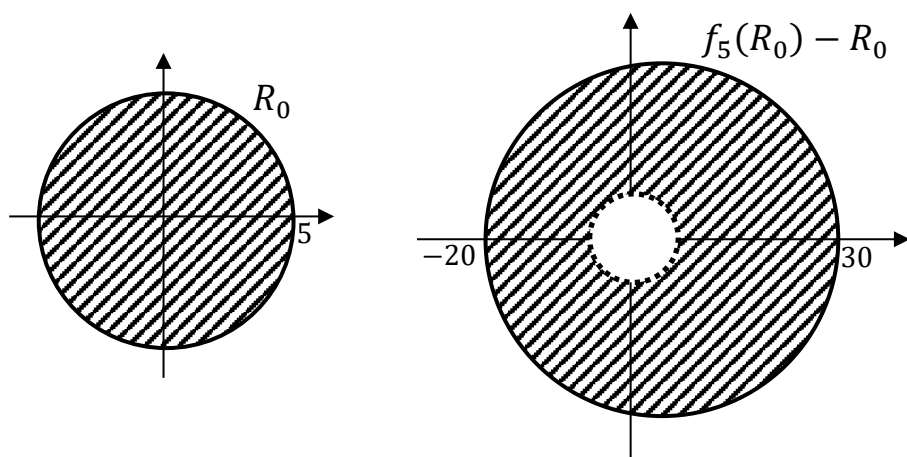


$H(z) = z + 1/z$ maps J_0 to J_{-2} and it maps rays out from J_0 to hyperbolas out from J_{-2} . More important, it conjugates J_0 on to J_{-2} .
 $H(z^2) = (H(z))^2 - 2 \rightarrow H \circ f_0 = f_{-2} \circ H$

This shows that the dynamics of one case is mirrored in the dynamics of the other case and even more importantly this relation between J_0 and J_{-2} can be extended (with other H) to all other fractal Julia sets.

The relation is stronger when J_c is connected as is the case for $c = -2$ and $c = 0$. As an example of a non-connected J_c let's look at $c = 5$. This will hold for all $|c| > 2$.

Start with Region $R_0 = \{z : |z| \leq 5\}$ which $f_5(z) = z^2 + 5$ maps into a disk of radius 25 centered at $z = 5$.



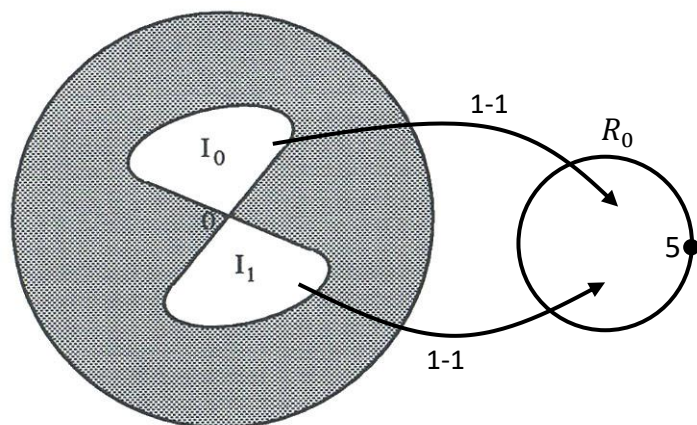
All points in the region $f_5(R_0) - R_0$ are mapped to the exterior of that region and their orbits escape to ∞ .

The prisoner set P_5 is the complement of points whose orbit enter $f_5(R_0) - R_0$.

Form the set $R_1 = \{z: f_5(z) \in R_0\}$, the set of preimages of R_0 .

$z = 5$ is the only one just one preimage ($z^2 + 5 = 5 \rightarrow z_{1,2} = 0$).

The other points have two preimages that form two lobes I_0 and I_1 that pinch together at $z = 0$, $R_1 = I_0 \cup I_1$.



Each lobe maps one-to-one onto R_0 .

The exterior of R_1 maps to $f_5(R_0) - R_0$ and escapes. R_1 is part of $R_0 \rightarrow$ there are subsets in each lobe that maps to R_1 , and just as before these preimages are two lobes pinched together.

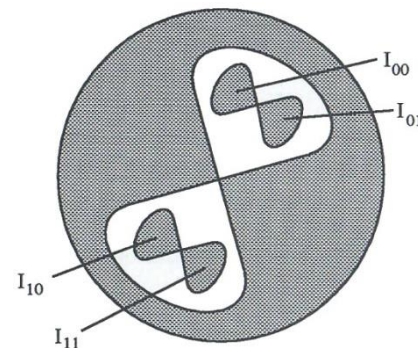
And so it goes on recursively $R_{n+1} = f_5^{-1}(R_n)$.

Prisoner set P_5 is the limiting nested set $\bigcap_{k=1}^{\infty} R_k$.

Each component approaches a single point as $k \rightarrow \infty$.

P_5 is a Cantor set and $J_5 = P_5$.

All Julia sets J_c with $|c| > 2$ are disconnected Cantor sets.



The argument above only really used the fact that the orbit of 0 escaped for f_5 .

This leads to two important theorems for quadratic polynomials and a natural definition of the Mandelbrot set.

Theorem

If the orbit of 0 escapes under iteration of f_c then the prisoner set equals the Julia set and J_c is a Cantor set.

Theorem

If the orbit of 0 does not escape under iterations of f_c then both P_c and J_c are connected sets.

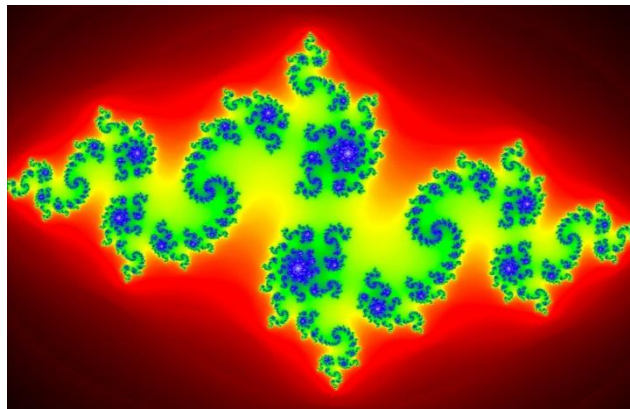
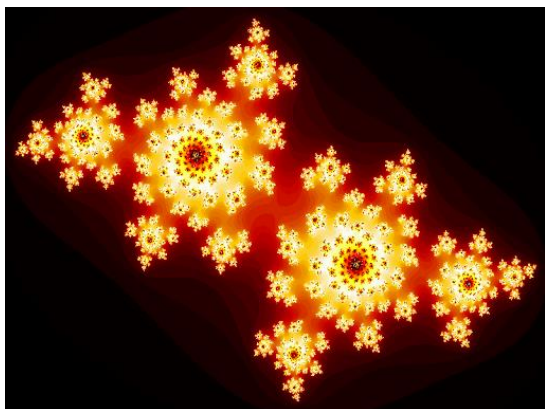
Definition

Parameters c for which the Julia set is connected is called the **Mandelbrot set** $M = \{c \in \mathbb{C} | J_c \text{ is connected}\}$

The theorems give an alternative definition that is easier to work with $M = \{c \in \mathbb{C} | f_c^k(0) \not\rightarrow \infty \text{ as } k \rightarrow \infty\}$.

This can be generalized to other functions by looking at orbits $\mathcal{O}(z_0)$ of the critical points where $f'(z_0) = 0$.

The critical orbits hold the key to the topological structure of the filled Julia sets P_c . An example of the importance of the critical orbit is that if f_c has an attracting periodic orbit then the orbit of 0 must be attracted to this orbit, which means that at most one of the periodic points can have an attracting orbit.



Disconnected Julia sets with different color-coding of the escape sets

Julia sets and Field lines

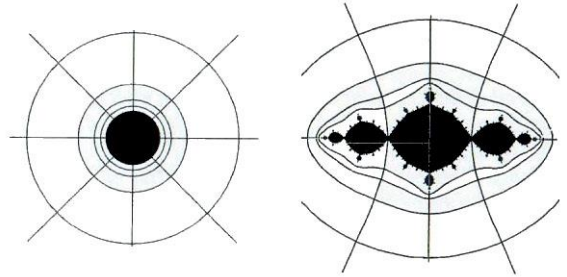
60 years after the work of Julia and Fatou in the beginning of the 1900's there was new progress in the study of Julia sets. This work used ideas from electrostatics and was done by Adrien Douady and John Hubbard.

When a metal plate is charged with electrons they spread out evenly over the surface and electric field lines give directions of force on a small charge placed outside the charged object. The field lines leave the object in straight angles and encode its shape. The equations for the electric field lines are a basic part of electrostatics.

The force fields of electrostatics are conservative, the work to move a charge around in a loop against and along the electric field is zero, $\oint q\vec{E} \cdot d\vec{s} = 0$ where $\vec{F} = q\vec{E}$ and \vec{F} is the force on a charge q in an electric field $\vec{E}(\vec{r})$.

In a conservative force field, you can introduce potential energy and equipotential surfaces where the potential energy per unit charge is the same ($1 J/C = 1 V$) and the work to transport a charge from A to B equals the difference in potential $V_{AB} = U_B - U_A$. The equations of electrostatics take place in three dimensions but the two-dimensional Julia sets and their interior can be extended in one dimension to a 3D-setting.

Equipotential surfaces and field lines are perpendicular. Surfaces and field lines can be viewed as part of a system of coordinates, in two dimension a polar coordinate system.

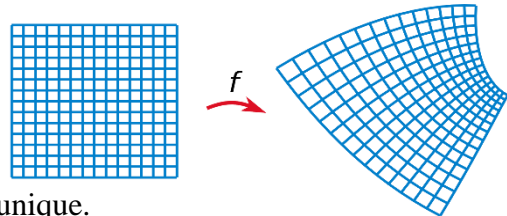


Douady's and Hubbard's work on Julia sets is based on the Riemann mapping theorem from complex analysis that states:

Riemann mapping theorem

If Ω is a non-empty simply connected (no holes) subset of \mathbb{C} then there is a **biholomorphic** mapping f , (f and f^{-1} are both **holomorphic** (complex differentiable)) from Ω onto the open unit disc.

That f is biholomorphic implies that it is **conformal**, locally preserving angles, which is described locally by a scaling factor and a rotation angle.

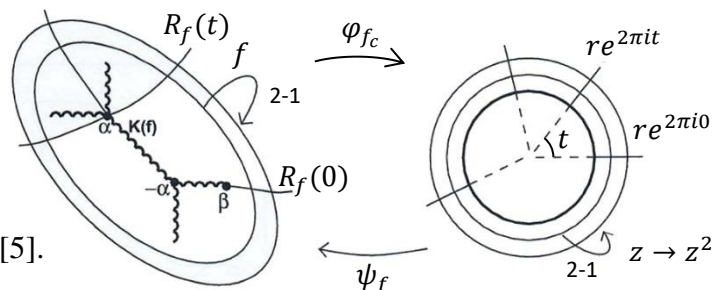


Later Henri Poincaré proved that the mapping is essentially unique.

To state the central fact of field lines and equipotentials I quote directly from article [19]:

“Let $f(z) = z^2 + c$ have a connected Julia set. Since the point at ∞ is a superattracting fixed point, the dynamics in its basin of attraction, $A(\infty)$ is very simple. One can find a holomorphic change of variables $\psi_f: \mathbb{C} \setminus \mathbb{D} \rightarrow A(\infty)$ called the **Böttcher coordinates** at infinity that conjugates $f|_{A(\infty)}$ to the map $z \rightarrow z^2$ on the complement of the closed unit disk. This change is unique if we require the derivative at infinity to be one. The image under ψ_f of a circle or radius $\exp(\eta) > 1$ in $\mathbb{C} \setminus \mathbb{D}$ is a simple closed curve in $A(\infty)$ called an **equipotential** of potential η ”.

“If we parametrize the arguments of the unit circle from 0 to 1, the image under ψ_f of a ray of argument t is called an **external ray** of argument t and denoted by $R_f(t)$ ”.



A proof of this is not very hard it can be read in reference [5].

Differentiability in \mathbb{C} vs. \mathbb{R}^2

To differentiate a function $f: \mathbb{C} \rightarrow \mathbb{C}$ with $x + iy \rightarrow u(x, y) + iv(x, y)$ is different from differentiating a function $g: \mathbb{R}^2 \rightarrow \mathbb{R}^2$ with $(x, y) \rightarrow (u(x, y), v(x, y))$

\mathbb{C} has more structure than \mathbb{R}^2 , complex numbers can be multiplied and divided, vectors can not.

$$f'(z) \equiv \lim_{\substack{h \rightarrow 0 \\ h \in \mathbb{C}}} \frac{f(z+h) - f(z)}{h} \quad \text{doesn't work in } \mathbb{R}^2 \text{ where } h \text{ would be a vector.}$$

Differentiating with $h = (\alpha, \beta)$ in two dimensions puts strict restrictions on u and v :

$$\lim_{\substack{\alpha \rightarrow 0 \\ \alpha \in \mathbb{R}}} \frac{f(z+\alpha) - f(z)}{\alpha} = \lim_{\substack{\beta \rightarrow 0 \\ \beta \in \mathbb{R}}} \frac{f(z+i\beta) - f(z)}{i\beta}$$

$$\frac{\partial f}{\partial x}(z) = \frac{1}{i} \cdot \frac{\partial f}{\partial y}(z)$$

$$\frac{\partial u}{\partial x} + i \frac{\partial v}{\partial x} = \frac{1}{i} \left(\frac{\partial u}{\partial y} + i \frac{\partial v}{\partial y} \right)$$

$$\begin{cases} \frac{\partial u}{\partial x} = \frac{\partial v}{\partial y} \\ \frac{\partial v}{\partial x} = -\frac{\partial u}{\partial y} \end{cases} \Rightarrow \begin{cases} \frac{\partial^2 u}{\partial x^2} + \frac{\partial^2 u}{\partial y^2} = 0 \\ \frac{\partial^2 v}{\partial x^2} + \frac{\partial^2 v}{\partial y^2} = 0 \end{cases}$$

$$\begin{cases} \nabla^2 u = 0 \\ \nabla^2 v = 0 \end{cases}$$

Equipotential curves of u and v are orthogonal
 \uparrow
 CR $\Rightarrow \nabla u \cdot \nabla v = 0$

Cauchy-Riemann equations (CR)

Laplace equations

If certain conditions of continuity and differentiability are satisfied then the Cauchy-Riemann equations are a necessary and sufficient condition for complex differentiability.

CR expresses a geometric condition on the Jacobian matrix of the partial derivatives, $f(z)$ is locally a composition of a rotation with a scaling and thereby a preservation of angles. CR is the condition on f to be a conformal mapping.

Back to Julia sets and field lines, starting with $c = 0$ and the prisoner set $P_0 = \{z: |z| \leq 1\}$. The field lines are radial lines emanating from P_0 , they can be labelled by the polar angle $\alpha \cdot 2\pi$ with $0 \leq \alpha < 1$.

The dynamics of $z \rightarrow z^2$ is represented by an iteration of the field lines $\alpha \rightarrow 2\alpha \pmod{1}$, the shift function. The function is best illustrated with $\alpha \in [0,1[$ in binary form $0.b_1b_2b_3 \dots$ where $b_k \in \{0,1\}$.

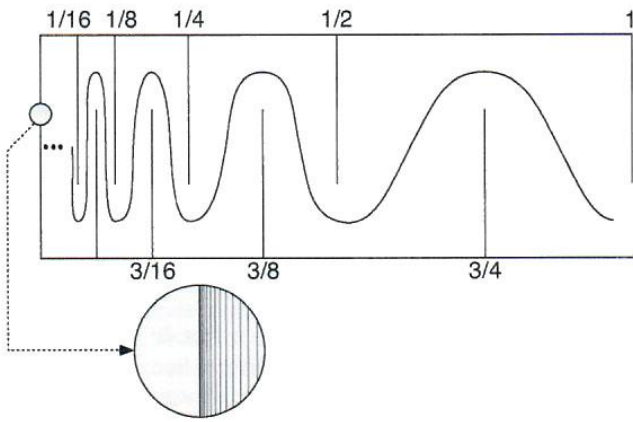
$$\alpha \in \mathbb{Q} \rightarrow \alpha = 0.d_1d_2 \dots d_l \overline{d_{l+1} \dots d_{l+m}} \quad 1/2 = 0.1\bar{0} \quad 1/3 = 0.\overline{01} \quad 2/3 = 0.\overline{10} \quad 1/6 = 0.0\overline{01}$$

With a preperiodic part $d_1d_2 \dots d_l$ and a periodic part of period $m, \overline{d_{l+1} \dots d_{l+m}}$.

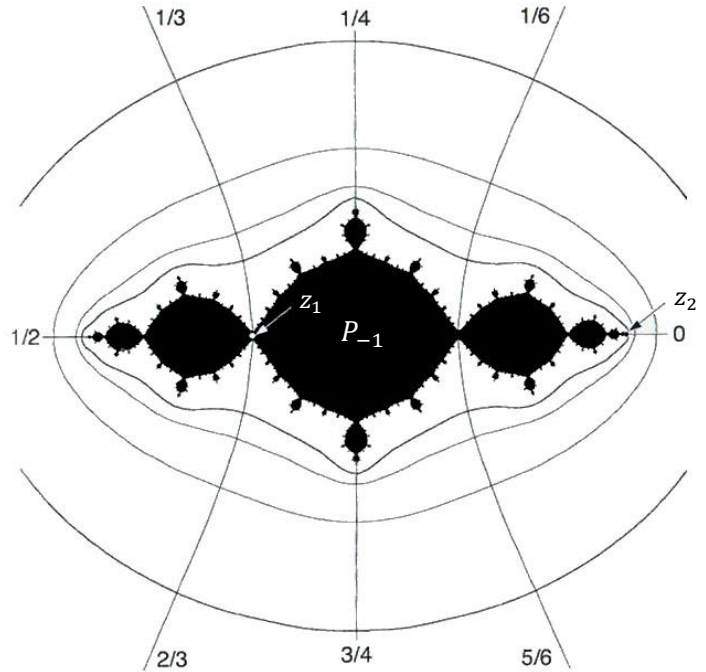
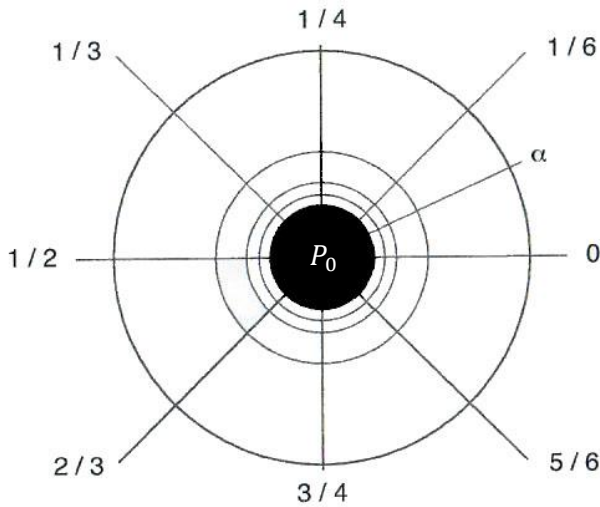
The dynamics in the radial direction is represented by equipotential surfaces labelled by the work of moving a charge from one level to another according to the rules of electrostatics when charges are spread over P_c and extended indefinitely into an extra dimension. For P_0 this is an infinite cylinder of uniform thickness.

The force field around a charged sphere weakens as $F \propto r^{-2}$ and the potential energy becomes $\int F dr \propto r^{-1}$. For an infinite cylinder $F \propto r^{-1}$ and the potential $\int F dr \propto \log r$ becomes logarithmic, $p(z) = \log |z|$.

If the Julia set is locally connected then each external ray lands on a unique point in J_c , the angle of the ray is the border points **external angle**. This is the case if 0 is preperiodic or if f_c has an attracting cycle. Not all Julia sets are locally connected so rays might not land. External angles tell about topology and dynamics of J_c .



The double comb connected in one end is an example of a connected shape that is not locally connected. It shows why an external ray to a locally non-connected shape need not have a unique limit point to land on.



Assignment of α to different field lines when $c = -1$. The Julia set J_0 has one repelling fixpoint at $z = 1$ where the field line $\alpha = 0$ lands. The $\alpha = 0$ field line in J_1 should correspond to a repelling fixpoint of $z \rightarrow z^2 - 1$.

$$z = z^2 - 1 \rightarrow \begin{cases} z_1 = (1 - \sqrt{5})/2 & |f'(z_1)| > 1 \\ z_2 = (1 + \sqrt{5})/2 & |f'(z_2)| > 1 \end{cases} \quad \text{Both are repelling.}$$

Symmetry under reflection in the real axis when $Im(c) = 0$ gives the invariant field line $\{z = x | x \geq z_2\}$.

What happens to the field line that ends in the other repelling fixpoint z_2 ?

That field line can't be invariant since that position is already taken by the field line of z_2 .

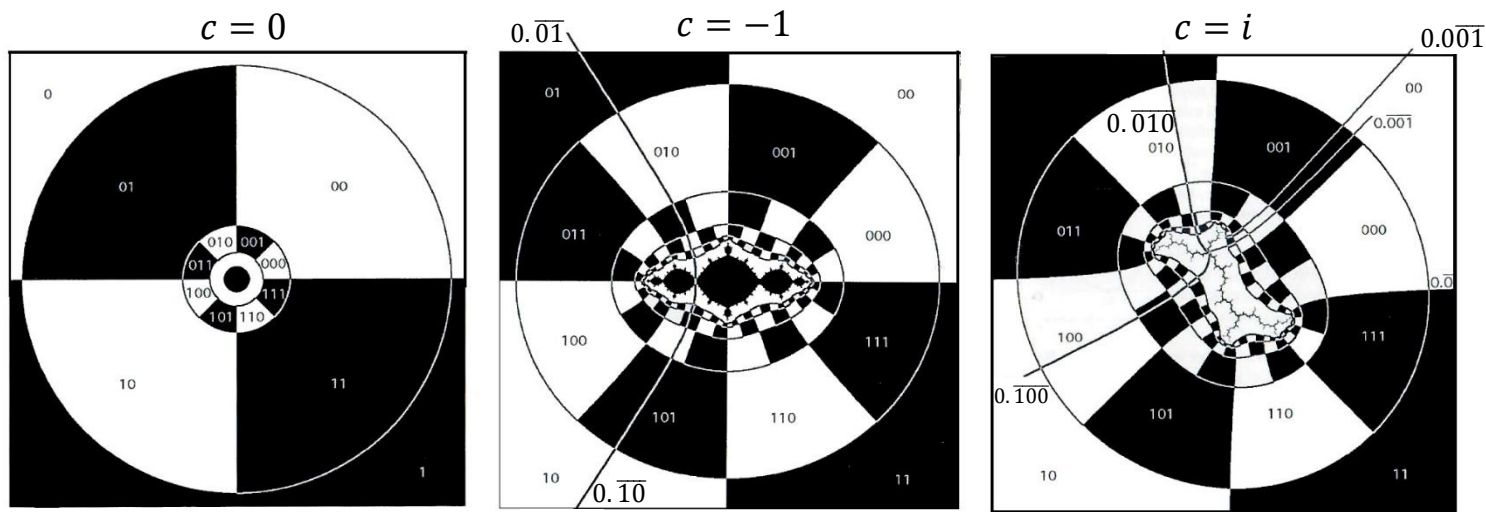
The dilemma is solved by having two field lines meet at z_2 and becoming part of a 2-cycle.

This can be done if the prisoner set P_{-1} is pinched at z_2 which happens to be the case as the figure shows.

$$\text{For two field lines to be part of a 2-cycle means } \begin{cases} 2\alpha_1 \pmod{1} = \alpha_2 \\ 2\alpha_2 \pmod{1} = \alpha_1 \end{cases} \text{ which is solved by } \begin{cases} \alpha_1 = 1/3 \\ \alpha_2 = 2/3 \end{cases}$$

To find the field line having $\alpha = 0$ in the general case when $Im(c) \neq 0$ can be done by starting from a great distance from which the Julia set looks like a point charge and the equipotential curves become big circles centered $z = 0$. The position of $\alpha = 0$ is found by backtracking curve segments starting at the positive real axis.

The work of Douady and Hubbard showed that for a connected Julia set there is a one-to-one correspondence that translates the dynamics, equipotentials and field lines of $z \rightarrow z^2$ to the corresponding ones in $z \rightarrow z^2 + c$. The angle of each field line encodes the segments that it passes through on its way to the boundary J_c .



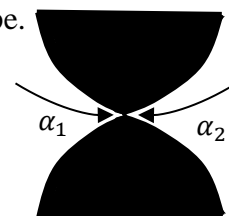
Binary decomposition of the escape set from equipotential lines and external rays.

The shape of a Julia set or its interior P_c can be understood by analysing the pinch points of field lines. Start from P_0 , a disk and whenever n field lines meet, pinch them together to change the shape. The pinch points in P_{-1} of pairs of field lines is the result of iterated pre-images of z_1 .

An example with 3 field lines coming together can be seen in P_i .

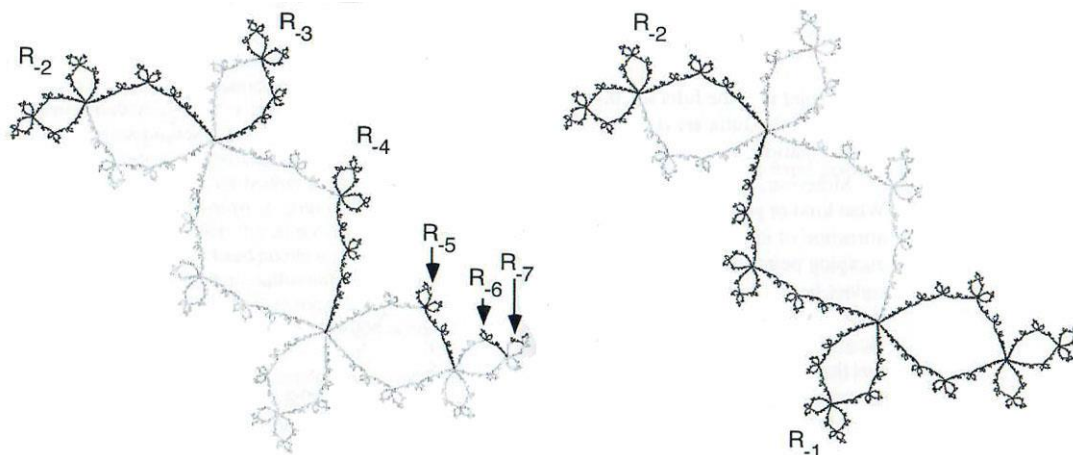
The fixpoints of $z \rightarrow z^2 + i$, $z = z^2 + i$ are $z_{1,2} = (1 \pm \sqrt{1 - 4i})/2$.

One of which corresponds to $\alpha = 0$ and the other corresponds to a pinch with 3 field lines.



$$\begin{aligned} \alpha_2 &= 2\alpha_1 \pmod{1} \\ \alpha_3 &= 2\alpha_2 \pmod{1} \\ \alpha_1 &= 2\alpha_3 \pmod{1} \end{aligned} \quad \text{with solution } \begin{cases} \alpha_1 = 1/7 = 0.\overline{001} \\ \alpha_2 = 2/7 = 0.\overline{010} \\ \alpha_3 = 4/7 = 0.\overline{100} \end{cases}$$

Another example of a J_c with pinch points where 3 field lines come together is $J_{-0.12+0.74i}$ a.k.a. 'the rabbit'.



The **self-similarity** of a Julia set is not exact. When a part of an image is replicated on a larger or smaller scale it is transformed by $z \rightarrow z^2 + c$ to something similar but not an exact copy, $R_{-7} \rightarrow R_{-6} \rightarrow \dots \rightarrow R_{-1}$. Another transformation and R_0 will yield the whole Julia set.

Take any small subset of a Julia set and apply $z \rightarrow z^2 + c$ to every point and iterate and you will eventually get back the complete Julia set.

The Mandelbrot set, its history and appearance

Everything starts from something else. A history of the Mandelbrot set could start with Sir Artur Cayley in 1879 when he wrote about basins of attraction for different roots when using Newton's method to solve $z^3 = 1$.

The boundary of the basin of attraction is named after Gaston Julia (1893 – 1978) who was inspired by Cayley's work. Pictures of Gaston show him wearing a mask. He lost his nose during a meaningless attack by German forces to celebrate the Kaiser's birthday during WW I. He had to wear a leather strap across his face after that. While recovering from the war wounds in an army hospital he studied the mathematics of Julia sets.

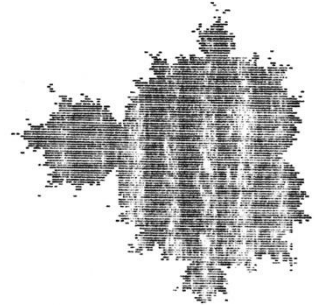
The complement of the filled Julia set is named after Pierre Fatou (1878 – 1929), a colleague and contestant to Julia who made many important contributions in complex analysis and specially on complex iterations. Julia and Fatou had no access to computer generated images of the sets they studied. Their results were almost forgotten. It took 60 years and the arrival of computers and computer-generated images before there was a new interest to study the sets of Julia and Fatou. This field is now a part of mathematics called complex dynamics.

Julia sets J_c are either connected or disconnected. The methods of the previous sections only apply to connected Julia sets which makes it interesting to study the set $\mathbb{M} = \{ c \mid J_c \text{ is connected} \}$.

The first image of \mathbb{M} is from 1978 by Robert Brooks and Peter Matelski from a study of Klein groups. IBM researcher Benoit Mandelbrot presented the set in a 1980 article on quadratic polynomials and made it known to a wider audience in a series of books that popularized the study of self-similarity, in both nature and mathematics. It was Mandelbrot who introduced the term fractal for highly irregular and self-similar shapes.

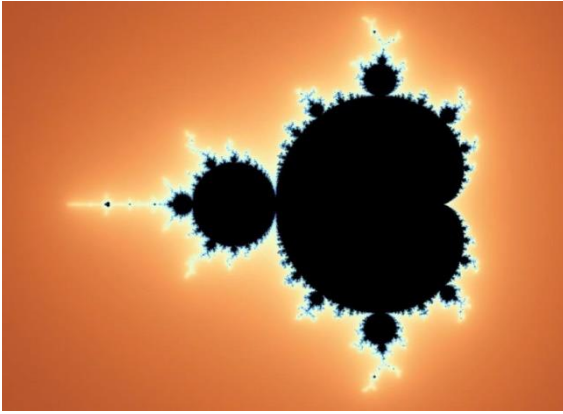


Early images of \mathbb{M} .
The left one by Brooks and Matelski.
The right one by Mandelbrot.



Much of the theory behind the set and its mathematical properties were revealed in the mid 80's by Adrien Douady and his student John Hubbard. They named the set after Mandelbrot.





The Mandelbrot set has a main part shaped like a **cardioid**. Onto this are attached circular **bulbs** and on these bulbs are more bulbs in an infinite regress. The attaching point of a bulb we can call **pinch point** or **root** of the bulb.

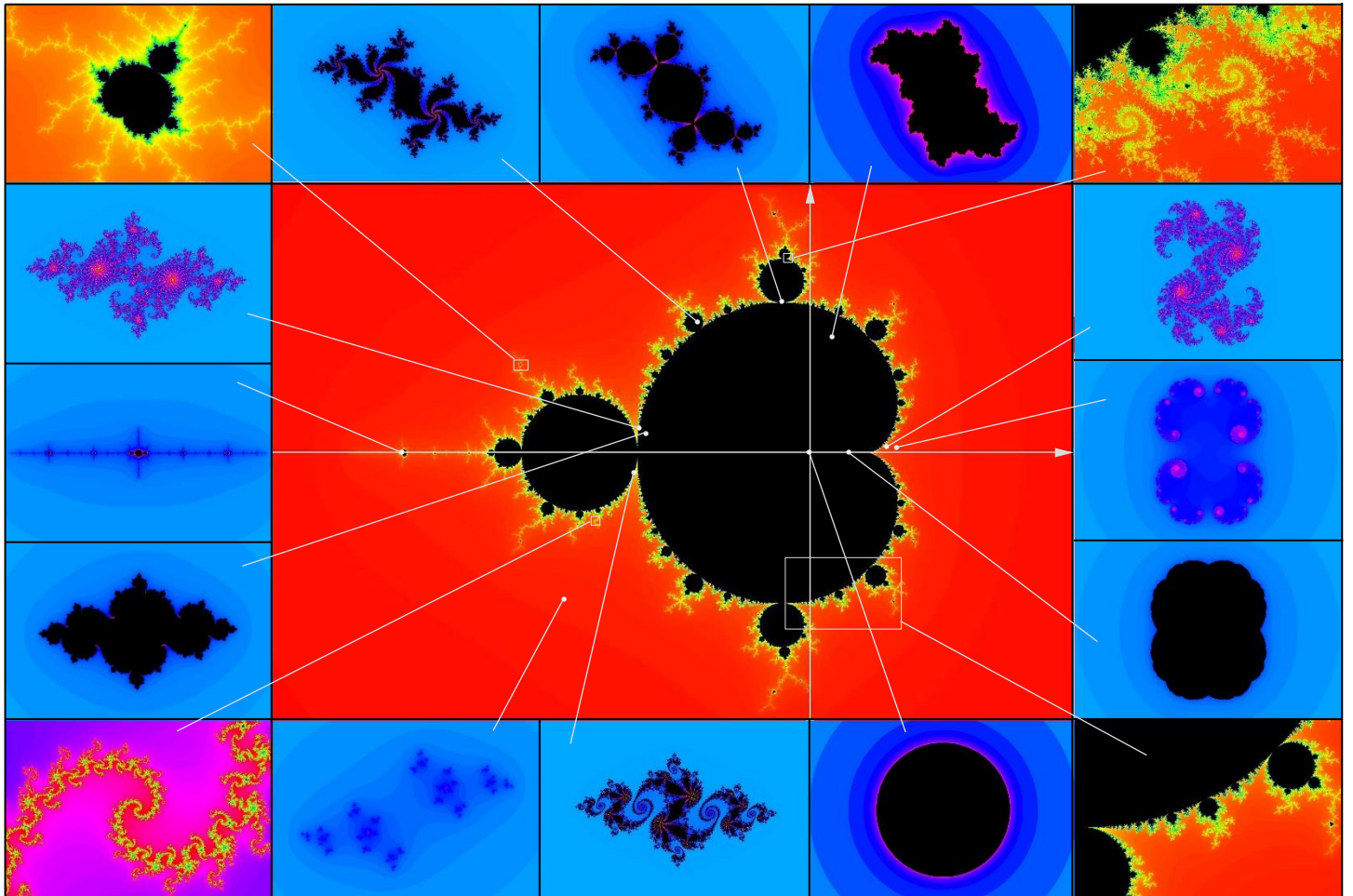
The small black dots in the image turn out to be miniature copies of the whole Mandelbrot set. Each miniature copy is attached to the main body by a unique filamentary network so there is no exact self-similarity, every copy is a slightly altered version of the main body.

The Mandelbrot set and the Julia set live in different worlds.

The Julia sets live in z -space, there is one Julia set for each value of c .

If $\mathcal{O}_{f_c}(z) = z, f_c(z), f_c^2(z), \dots$ is bounded then z is part of the prisoner set P_c with Julia set $J_c = \partial P_c$.

The Mandelbrot lives in c -space, the parameter space and each point represents a different iteration $z \rightarrow z^2 + c$. If J_c of that iteration is connected then c belongs to \mathbb{M} .



This picture shows the Mandelbrot set, $-2.25 \leq c_{\text{Re}} \leq 1.25$ and $-1.15 \leq c_{\text{Im}} \leq 1.15$ with enlargements from different locations in the corner images. The black parts in the blue pictures are prisoner sets for different c . For areas outside \mathbb{M} the Julia sets are just Cantor sets of disconnected points, **Cantor dust** so there you can't really see the black parts. The c -value of each Julia set is indicated by pointers to \mathbb{M} and its surroundings. Each Julia image covers the same z -area in the complex plane, $z_{\text{Re}} \in [-2, 2]$ and $z_{\text{Im}} \in [-1.3, 1.3]$.

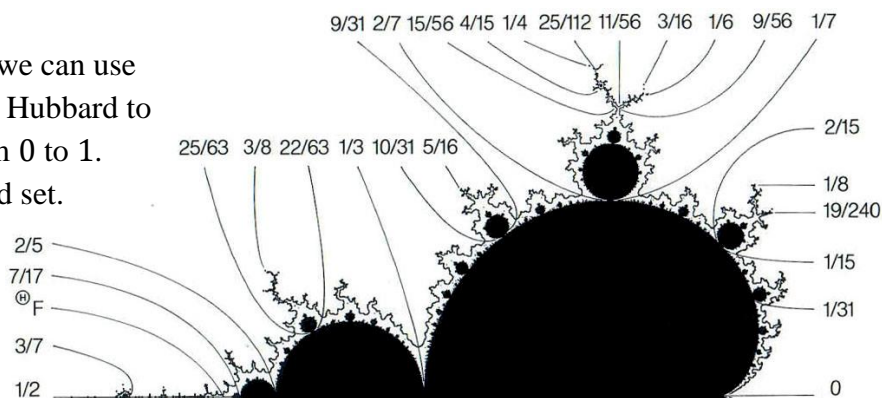
To understand the reflection symmetry of \mathbb{M} in the real axis we use the alternative definition of \mathbb{M} based on the theorem that J_c connected \Leftrightarrow orbit of critical point which is 0 does not escape under iterations with f_c . Based on $0 = \bar{0}$ and $\mathcal{O}_{f_{\bar{c}}}(\bar{z}_0) = \overline{\mathcal{O}_{f_c}(z_0)}$ it follows that the orbits under f_c are $f_{\bar{c}}$ are similar with regards to escaping so the membership in \mathbb{M} of c and \bar{c} is the same.

If the Mandelbrot set itself is connected then we can use the technique of external rays by Douady and Hubbard to attach numbers along the perimeter of \mathbb{M} from 0 to 1.

This method also proves that \mathbb{M} is a connected set.

In technical terms with $\varphi_{f_c}(z)$ from earlier.

$\Phi(c) \equiv \varphi_{f_c}(c)$ is an analytic isomorphism, from $\mathbb{C} - \mathbb{M}$ onto $\mathbb{C} - \mathbb{D}$ which shows that \mathbb{M} is a connected set.



Showing off of \mathbb{M}

Colorful pictures of the Mandelbrot set with surroundings are common in popular culture and popular science. These pictures are based on an algorithm that for each c calculates the number of iterations $f_c^k(0)$ it takes to reach a certain escape limit. If the limit is not reached before k reaches some maximum k_{\max} then c is assumed to be part of \mathbb{M} . Larger k_{\max} means higher resolution. As you zoom in on $\partial\mathbb{M}$ to see finer and finer details the bigger you must set k_{\max} . The number of iterations before the limit is reached is color-coded, an indication of closeness to \mathbb{M} . The color-coding has more to do with aesthetics than mathematics.

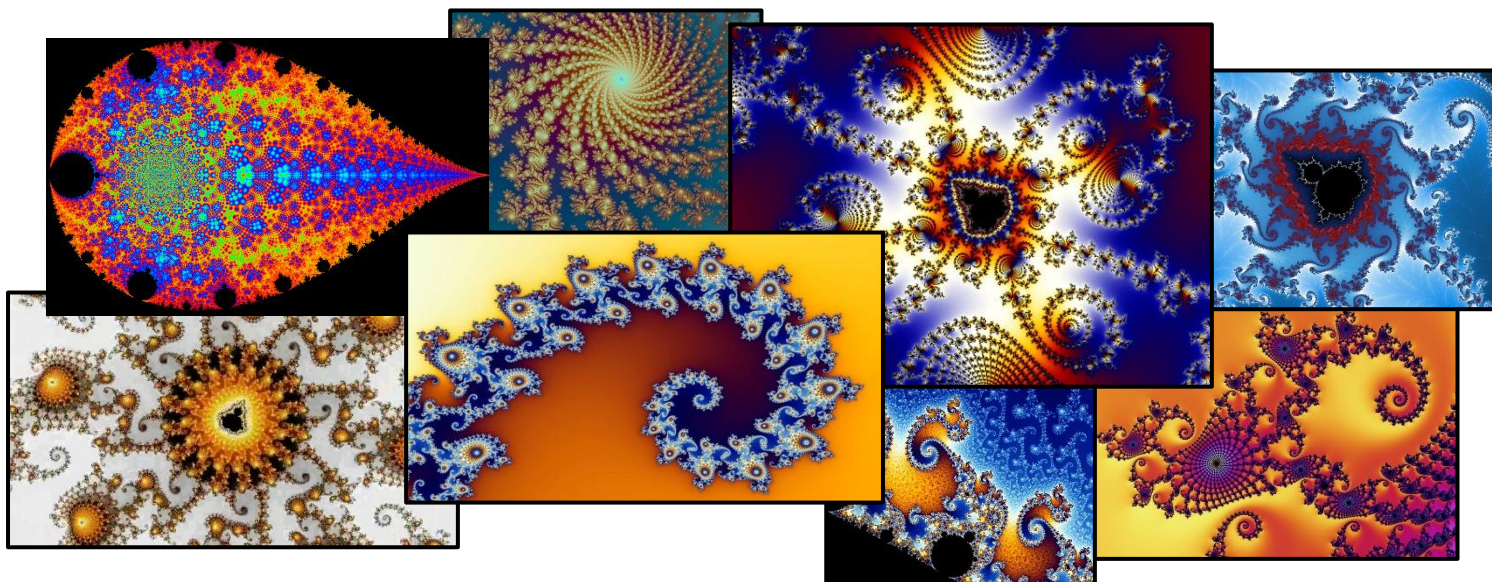
The application MANDELBROT on the menu starts with iterations confined to real numbers for z and c .

This makes it possible to see a diagram of $\lim_{k \rightarrow \infty} f_c^k(0)$ as a function of c without having to see 4-dimensionally.

In the Mandelbrot section of the application you can experiment with different resolutions k_{\max} and different color settings. You can set the view window, zoom in and out, do a zoom-rectangle with the mouse and look at the Julia set at a chosen location by right clicking with the mouse. The switch button $\boxed{\rightleftharpoons}$ gives you the Julia set in a big view where you can zoom in on chosen parts.

There are many apps for computers and mobiles that are much better and faster at showing the Mandelbrot set.

I settle with giving [this link](#) from Youtube with an animation that zooms in by a factor going from 1 to 10^{227} .



Periodic points

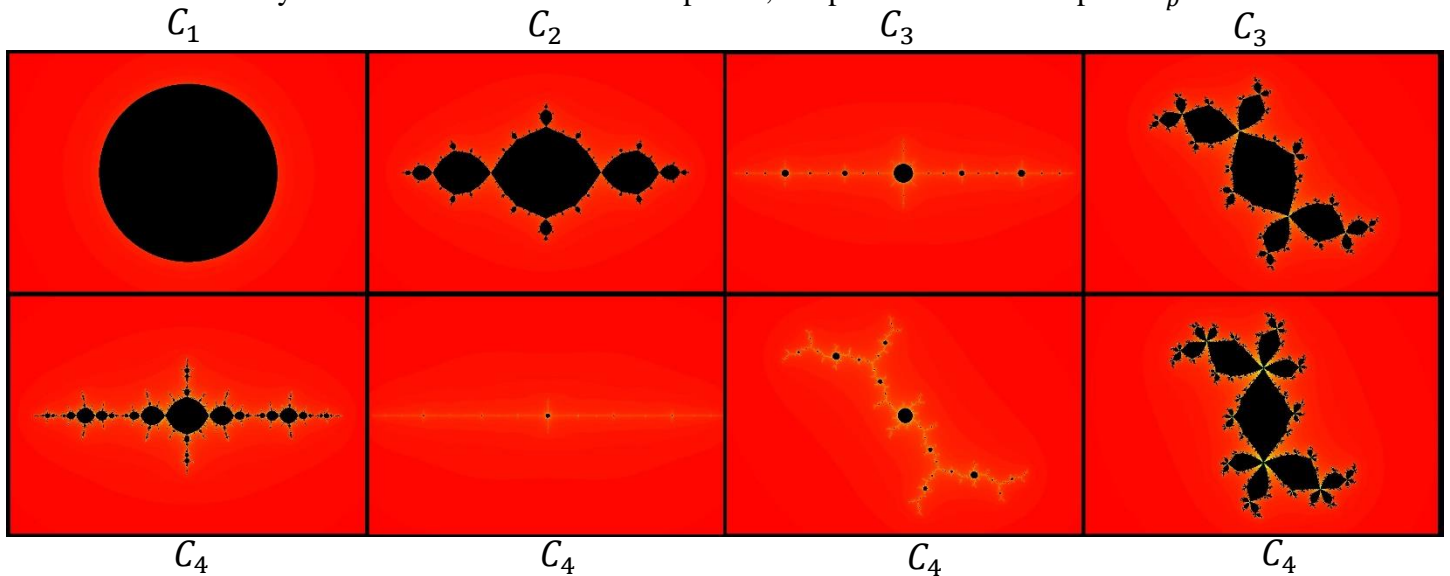
If the critical orbit $\mathcal{O}_{f_c}(0) = (f_c^k(0))_{k=0}^\infty = \underbrace{0}_{z_0}, \underbrace{c}_{z_1}, \underbrace{c^2+c}_{z_2}, \underbrace{(c^2+c)^2+c}_{z_3}, \underbrace{((c^2+c)^2+c)^2+c}_{z_4}, \dots$

is a loop with $z_p = z_0$ then it will not escape and $c \in \mathbb{M}$. Such c -points are called **periodic** of **period** p .

What values do they have, where are they on the Mandelbrot set and what do their Julia sets look like?

$p = 1 \quad c = 0$	$C_1 = 0$ (Solves $z_p = z_0$ for all $p > 1 \rightarrow$ discard $c = 0$ for $p > 1$)
$p = 2 \quad c^2 + c = 0$	$C_2 = -1$ (discard $c = -1$ when $p > 2$ and a multiple of 2)
$p = 3 \quad (c^2 + c)^2 + c = 0$	$\begin{cases} C_3 = -1.75488 \\ C_3 = -0.12256 \pm 0.74486i \end{cases}$ (discard when $p = 3k > 3$)
$p = 4 \quad ((c^2 + c)^2 + c)^2 + c = 0$	$\begin{cases} C_4 = -1.3107 \\ C_4 = -1.9408 \\ C_4 = -0.15652 \pm 1.03225i \\ C_4 = 0.28227 \pm 0.53006i \end{cases}$ (discard when $p = 4k > 4$)
$\vdots \quad \vdots$	\vdots

Plotting them on the Mandelbrot set shows that $c_{1,1}$ is at the centre of the cardioid and that the rest are centres of different bulbs. Every bulb can be associated with a period, the period of its centre point c_p .



Notice that for non-real c there will be pinch points in J_{c_p} where p shapes called **petals** come together in a point.

The main heart-shaped region of \mathbb{M} is defined by f_c having a single attracting fixed point. The fix-point lies in a prisoner set that goes from a circle at $c = 0$ to shapes with ever more ragged boundaries but always in the shape of a deformed circle, a simple closed curve with fractal dimension: $1 + |c|^2/4 \log 2 + O(c^3)$ when $|c| \ll 1$.

The 'cardioid' body is defined by:

$$\begin{cases} f_c(z) = z & \text{(single fixpoint)} \\ |f_c'(z)| < 1 & \text{(attracting)} \end{cases} \rightarrow \begin{cases} z^2 + c = z \\ |2z| < 1 \end{cases} \rightarrow \text{Boundary defined by } c = b(\theta) = e^{i\theta}/2 - e^{2i\theta}/4 \quad \theta \in [0, 2\pi[$$

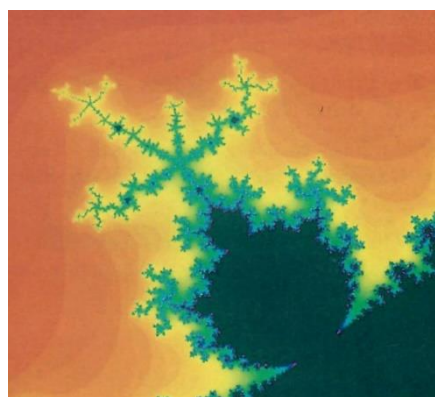
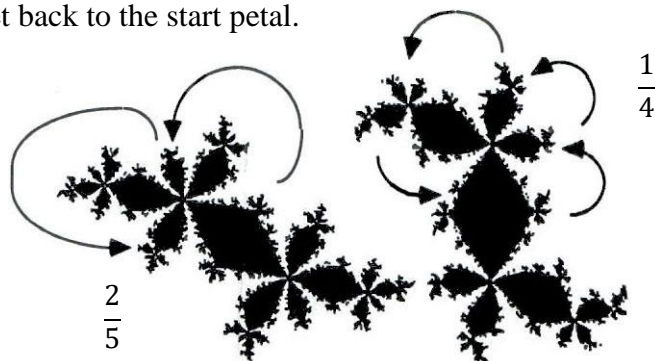
The body really is in the form of a cardioid, its inward pinch point is located at $c = b(0) = 1/4$. f_c has a neutral fix point at the cardioid boundary $f_c'(z) = e^{i\theta}$. The bulb to the left of the cardioid has an attracting cycle of period 2 defined by:

$$\begin{cases} f_c^2(z) = z \\ |f_c^{2'}(z)| < 1 \end{cases} \rightarrow \begin{cases} \text{Area bounded by} \\ |c + 1| = 1/4 \end{cases} \rightarrow \begin{cases} \text{A circle with radius } 1/4 \text{ centred at } c = -1 \\ \text{The boundaries meet at } c = -3/4 = b(\pi) \end{cases}$$

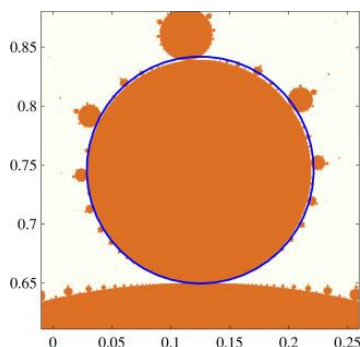
Each bulb is a circle described by the periodicity of its attracting cycle. There is also another number that characterizes each bulb. As c traverses the boundary of the cardioid and the derivative at the boundary point $f'_c(\theta)$ equals $e^{2\pi i \cdot p/q}$ we can expect a period q bifurcation when we pass from the cardioid into the bulb. The bulb attached at the pinch point is called a **p/q -bulb**. Every bulb has a filament growing out from it with a major branch point where q branches radiate outwards.

The numerator p determines the order in which the iterates jump between petals in the attracting cycle. Each iterate jumps p petals forward. Since p and q are relatively prime it will take q jumps before every petal has been visited once and the iteration has used p laps to get back to the start petal.

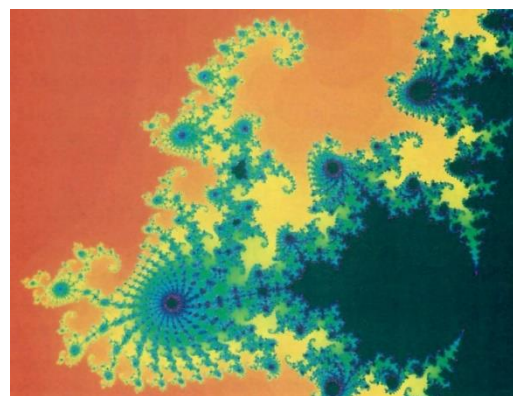
The numerator p determines the order in which the iterates jump between petals in the attracting cycle. Each iterate jumps p petals forward. Since p and q are relatively prime it will take q jumps before every petal has been visited once and the iteration has used p laps to get back to the start petal. The picture to the right shows the dynamics in P_c for $2/5$ -bulb and $1/4$ -bulb.



2/5 bulb



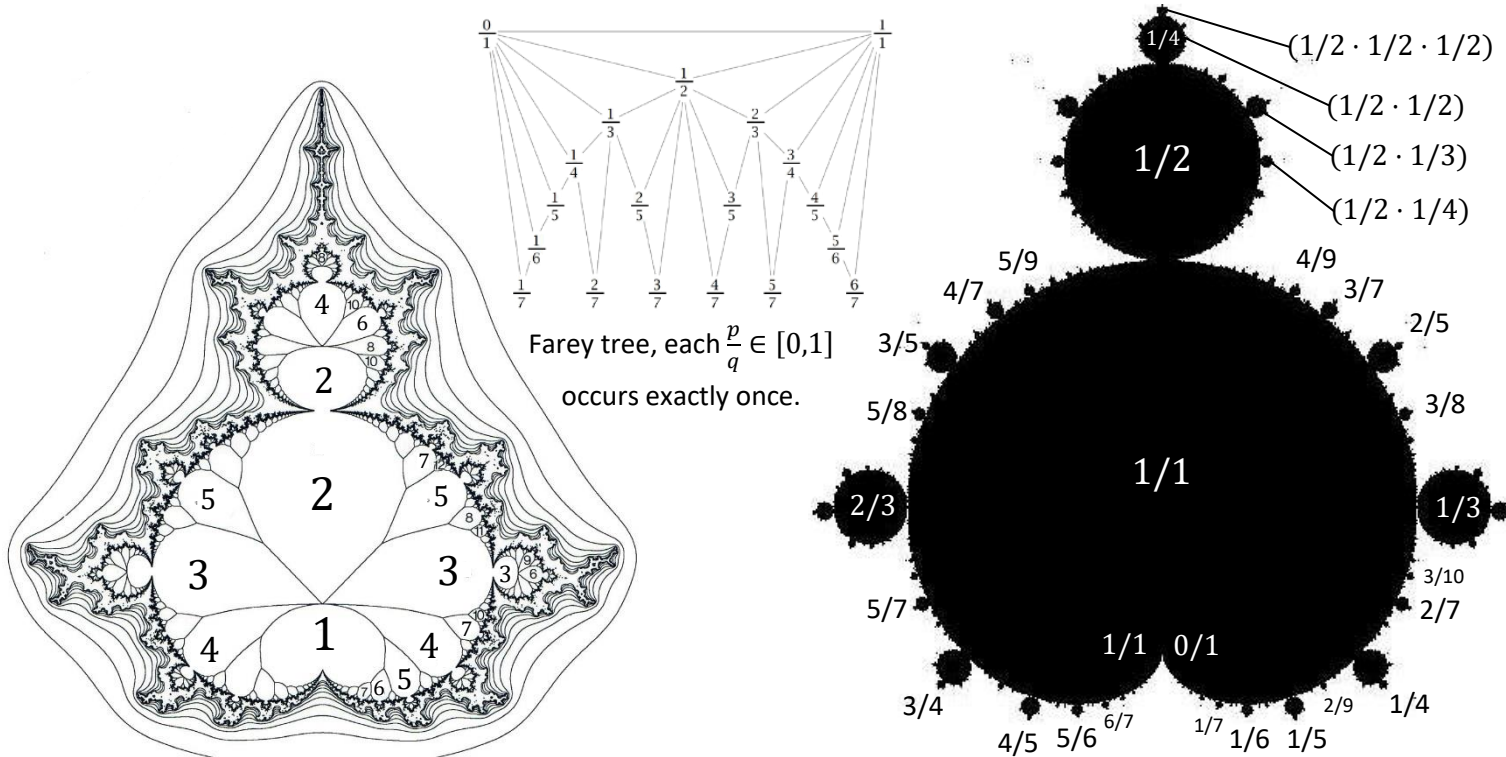
Bulbs are not exactly circular.
 $r(p, q) \approx q^{-2} \sin(\pi p/q)$



10/21 bulb

The ordering of p/q -bulbs along the perimeter follows a specific pattern, based on the Fibonacci sequence and

Farey addition where the biggest bulb on the cardioid between bulb a/b and bulb c/d is given by: $\frac{a}{b} \oplus \frac{c}{d} \equiv \frac{a+c}{b+d}$



Roots and Siegel disks

Every bulb has its own bulbs located around the perimeter in a similar manner. Points on the perimeter are specified by an **internal angle** $\alpha \in [0,1[$. We can focus on the main body with a single attracting fixed point and a cusp located at $\alpha = 0$. The cardioid is given by $c = \lambda/2(1 - \lambda/2)$ and $|\lambda| < 1$.

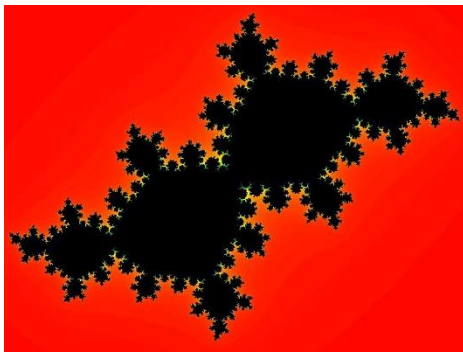
Satellite components are rooted at rational internal angles $\lambda = e^{2\pi i\alpha}$ with $\alpha = p/q$. At these positions the attractive fixed point turns into an indifferent cycle ($f' = 1$) that turns into an attractive cycle of period q .

$$p/q = 1/2 \rightarrow R_2 = -3/4$$

$$p/q = \pm 1/3 \rightarrow R_3 = (-1 \pm 3\sqrt{3}i)/8 = -0.125 \pm 0.6495i$$

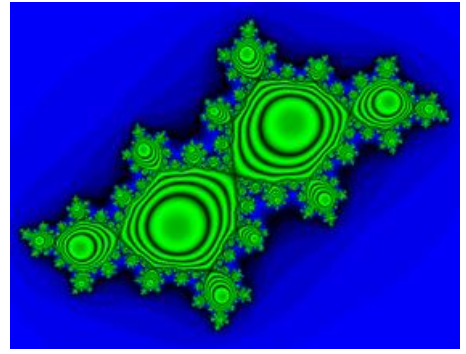
$$p/q = \pm 1/4 \rightarrow R_4 = 1/4 \pm i/2$$

When α is irrational and badly approximated by rationals, $\exists \epsilon, \mu > 0 \forall m, n: |\alpha - m/n| > \epsilon/n^\mu$ then the Julia set is of a special kind called a **Siegel disk**. The golden mean $\alpha = (\sqrt{5} - 1)/2$ is the 'most' irrational.



Siegel disk at $\alpha = (\sqrt{5} - 1)/2$
 $c = -0.3905 - 0.5868i$

Siegel disks have irrationally indifferent fixed points, neither attracting nor repelling. The blue figure shows orbits where an iteration is a rotation by angle α .



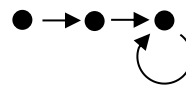
Preperiodic points

c -values are **preperiodic** if the critical orbit $z_0 = 0, z_1, z_2, \dots$ where $z_{m+1} \rightarrow z_m^2 + c$ starts with a sequence of length k that goes into a loop of period n , $z_k = z_{k+n}$. Such points $M_{k,n}$ are called **Misiurewicz points**. They are important when it comes to studying the dynamics of $f_c(z)$ and the Mandelbrot set. Since the critical orbit is stuck in a loop and can't escape, all these points belong to the Mandelbrot set.

Some examples of Misiurewicz points:

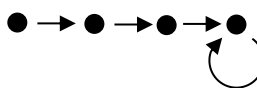
n. b. $\begin{cases} c = 0 & \text{are periodic} \\ c = -1 & \text{not preperiodic} \end{cases}$

$$k = 2 \quad n = 1 \quad \begin{aligned} c^2 + c &= (c^2 + c)^2 + c \\ 1 &= (c + 1)^2 \end{aligned}$$



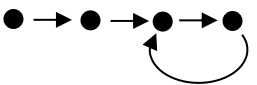
$$M_{2,1} = -2$$

$$k = 3 \quad n = 1 \quad (c^2 + c)^2 + c = ((c^2 + c)^2 + c)^2 + c$$



$$\begin{cases} M_{3,1} \approx -1.5437 \\ M_{3,1} \approx -0.228 \pm 1.115i \end{cases}$$

$$k = 2 \quad n = 2 \quad c^2 + c = ((c^2 + c)^2 + c)^2 + c$$



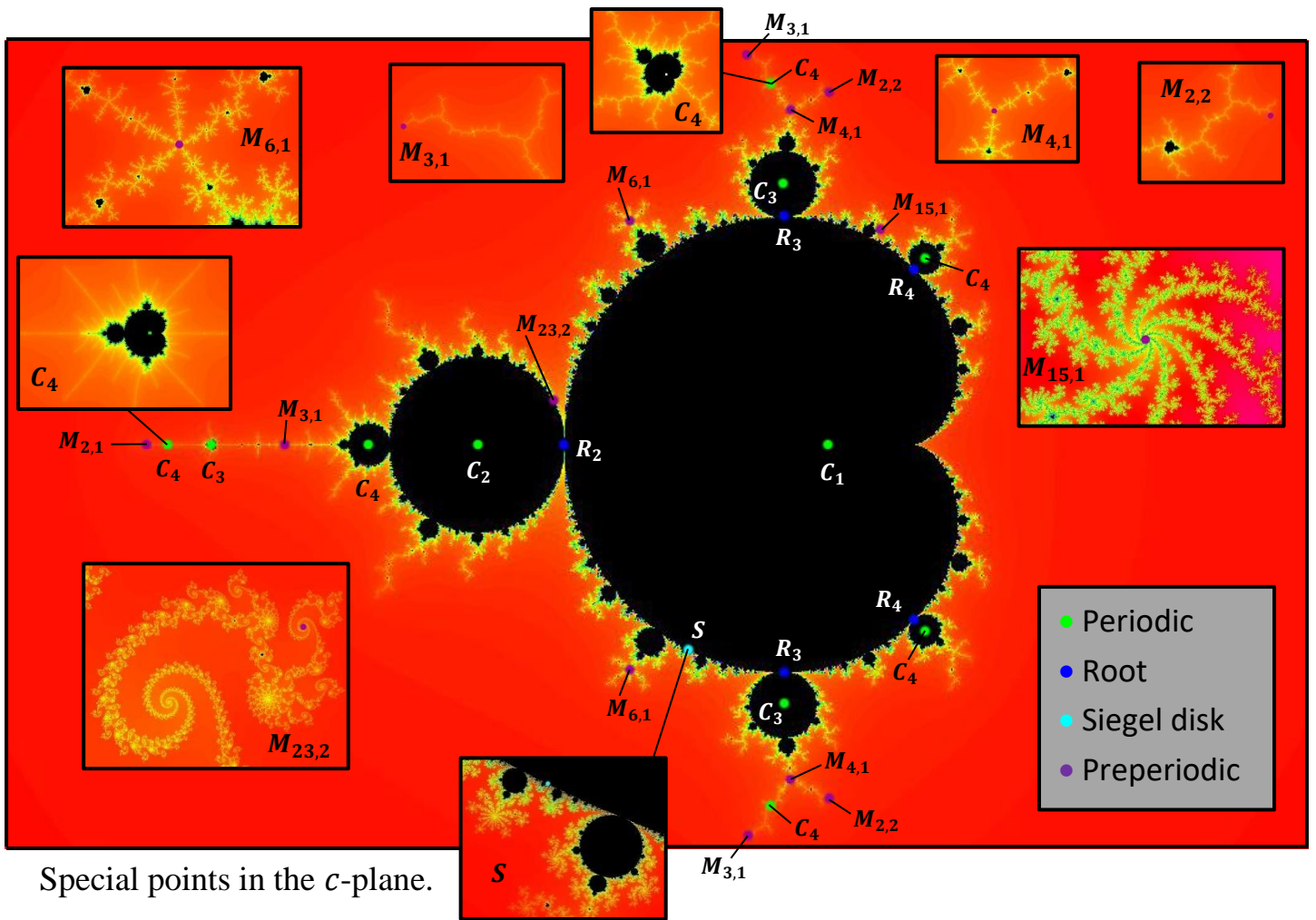
$$M_{2,2} = \pm i$$

$$c = -0.1010963 \dots + i \cdot 0.9562865 \dots \Rightarrow z_4 = z_5 \Rightarrow M_{4,1} \approx -0.101 + 0.956i$$

$$c = -0.562202 \dots + i \cdot 0.642817 \dots \Rightarrow z_6 = z_7 \Rightarrow M_{6,1} \approx -0.461 + 0.334i$$

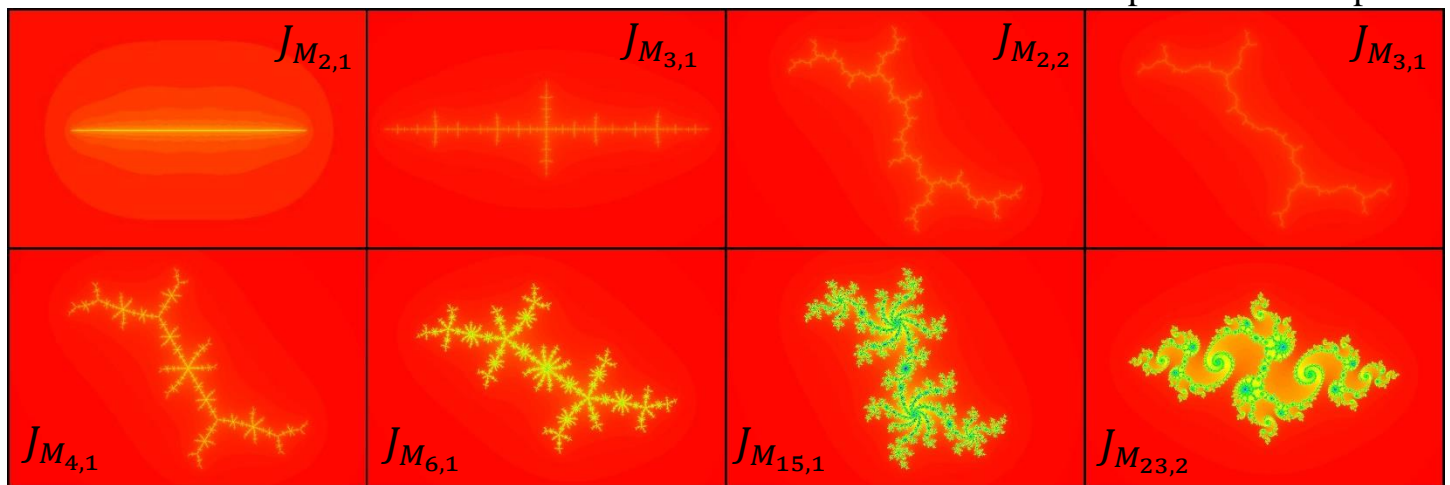
$$c = 0.1507200 \dots + i \cdot 0.6142203 \dots \Rightarrow z_{15} = z_{16} \Rightarrow M_{15,1} \approx -0.151 + 0.614i$$

$$c = -0.77568377 \dots + i \cdot 0.1364737 \dots \Rightarrow z_{23} = z_{25} \Rightarrow M_{23,2} \approx -0.757 + 0.136i$$



Special points in the c -plane.

Julia sets of Misiurewicz points in the z -plane.

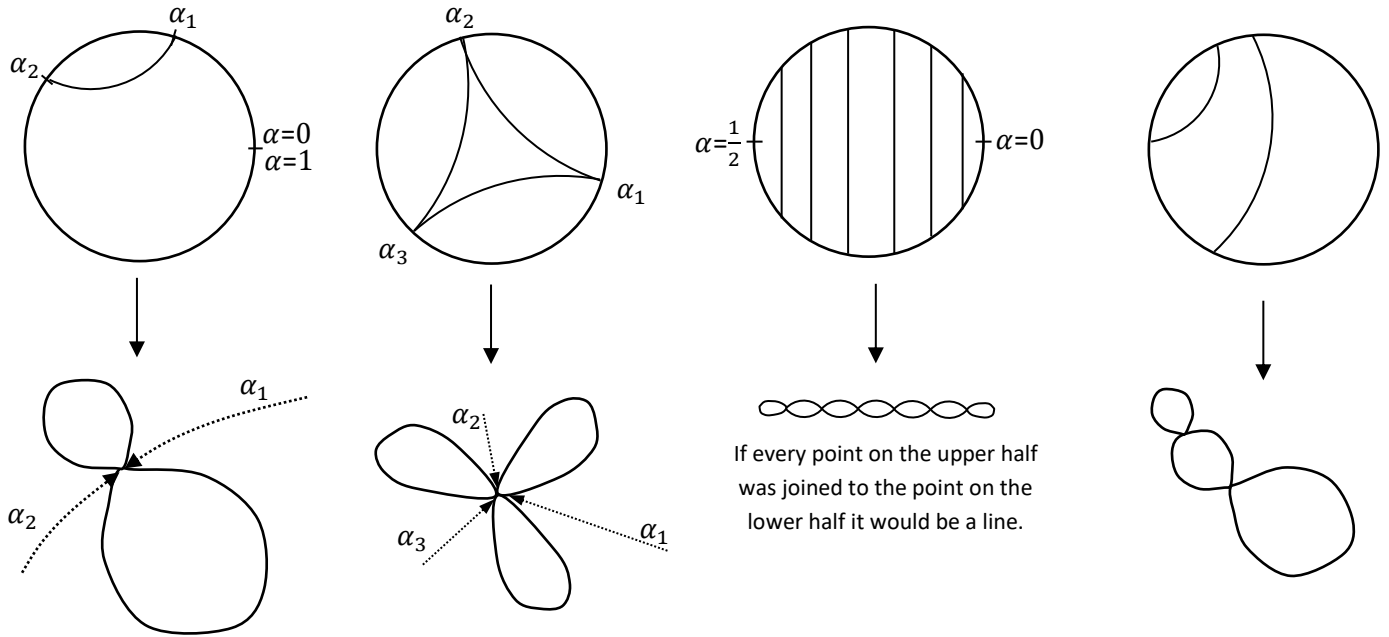


Notice how the preperiodic points are situated at **end of filaments**, at **center of spirals** or at **branchpoints**. The preperiodic points on the real line can be seen as branchpoints along the real line with two branches. Another very surprising fact is that the local appearance around a preperiodic point $M_{k,n}$ in the c -plane is replicated all over the Julia set J_c of the corresponding point $c = M_{k,n}$ in the z -plane. M and J_c are locally asymptotically self-similar around Misiurewicz points. Some other facts:

- The periodic n -cycle $z_k, z_{k+1}, \dots, z_{k+n-1}$ is repelling.
- They lie on the boundary and are dense on it. Every neighborhood of a point on ∂M contains a $M_{k,n}$ -point.
- The prisoner set equals the Julia set, which means that J_c has an empty interior with the form of an infinitely branched curve, a **dendrite**.
- They can be classified by the number of branches that come out from them, 1 for ends, 2 on filaments, 3 or more at branch points. The number equals the number of external rays.

External angles on external rays

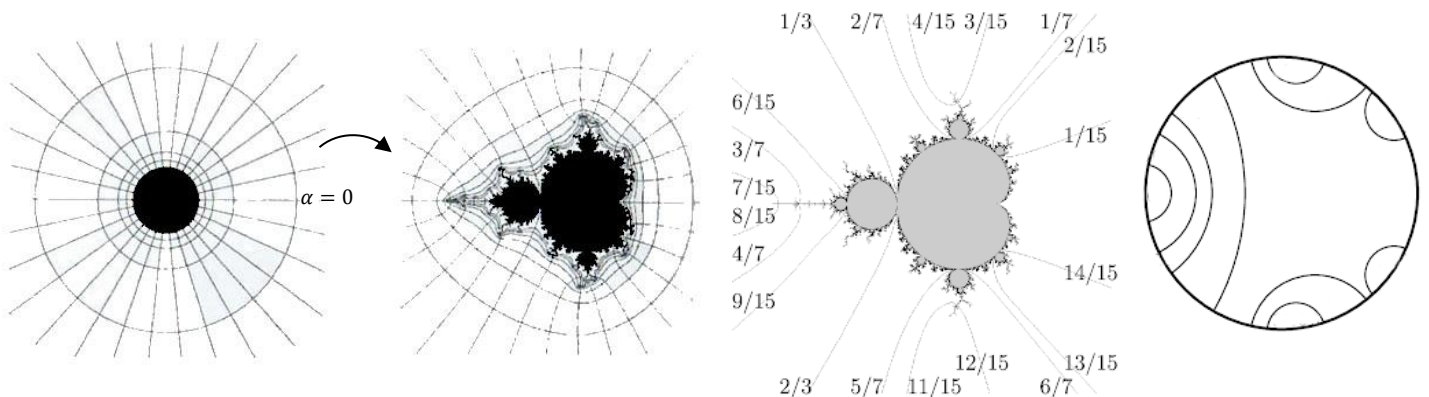
We have seen how external rays and external angles can be used on Julia sets to analyse them. At the point where an external ray reaches the boundary you put a value, the external angle $\alpha \in [0,1]$ corresponding to the asymptotic angle ($\alpha \cdot 360^\circ$) of the external ray. The external angles are marked on a circle and when several external rays land on the same point as in a pinch point or a branching it is marked by arcs joining these points. This gives an abstract representation of the shape of the set.



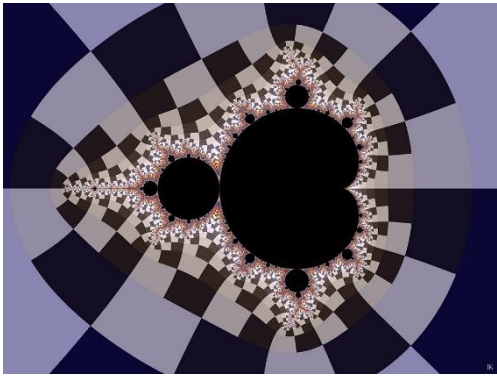
This method could be used on any connected set S but only if S is also locally connected are you guaranteed that every external ray can be extended to the boundary ∂S . Every Julia set is connected but there are some exceptional Julia sets that are not locally connected.

It has not been proved whether Siegel disks are locally connected but every irrational neutral fixed point that does not correspond to a Siegel disk is locally non-connected.

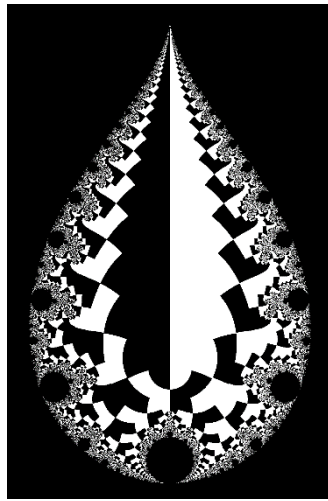
It's not known if the Mandelbrot set is locally connected but every ray corresponding to a rational number can be extended to $\partial \mathbb{M}$. $\alpha = 0$ corresponds to the cusp at $c = 0.25$. The reflection symmetry puts $\alpha = 1/2$ at the tip where $c = -2$ and every point on the real axis where two rays land must have $\alpha_1 + \alpha_2 = 1$.



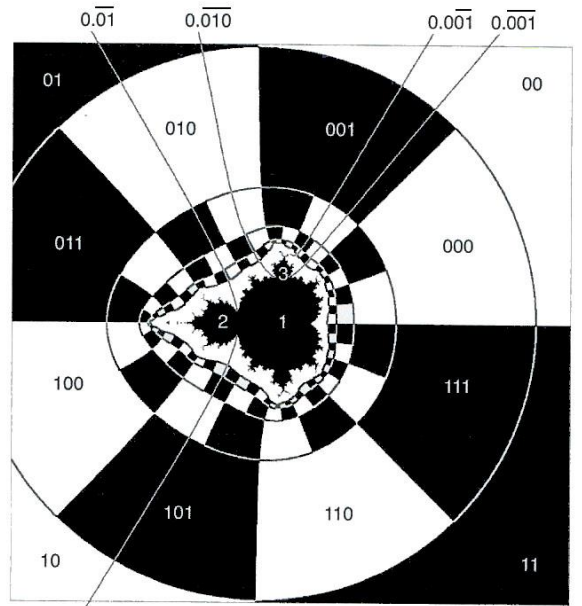
By using a polar orthogonal system with equipotential levels and external rays that we introduced for Julia sets we get a binary decomposition of the Mandelbrot exterior and a binary representation of α as we trace the external ray on its way to $\partial \mathbb{M}$.



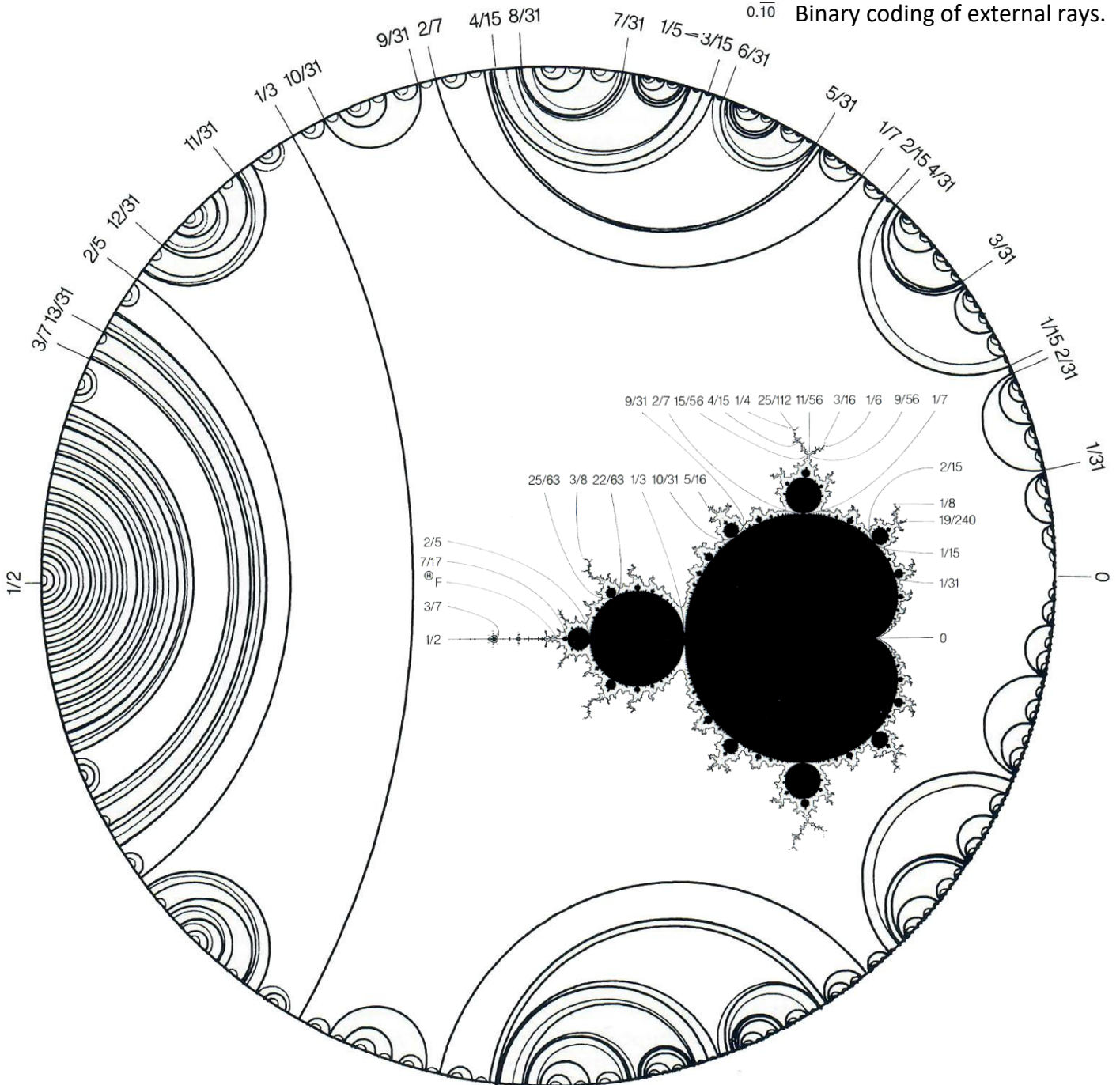
Binary decomposition of $\mathbb{C} \setminus M$.



Same thing in $1/c$ -plane.



Binary coding of external rays.



Model of the Mandelbrot set with external angles of roots and branchpoints on a circle.

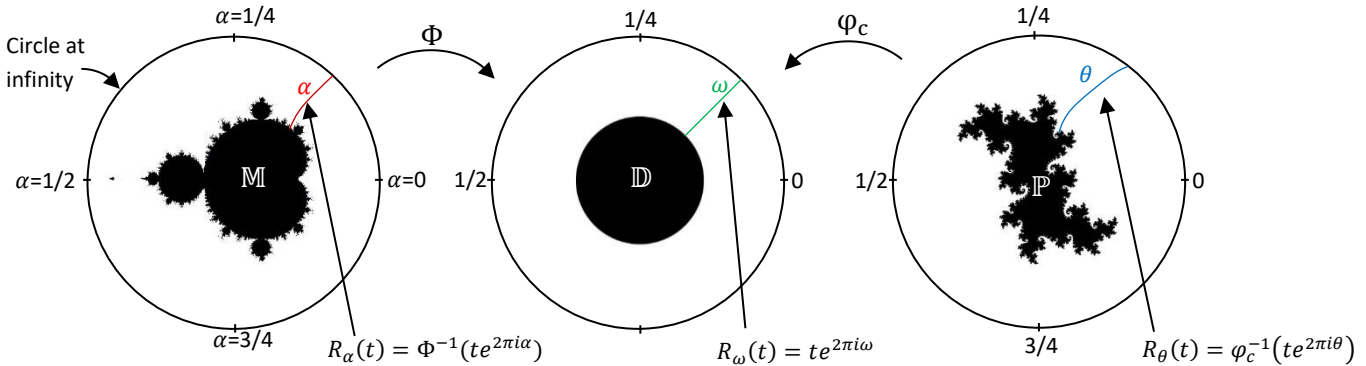
Calculating external angles on the Mandelbrot set

Start with the 'unique' analytic isomorphism $\varphi_c: \mathbb{C} \setminus \mathbb{M} \rightarrow \mathbb{C} \setminus \mathbb{D}$ that is responsible for polar coordinates around the filled Julia set J_c . The external rays are given by $R_\theta:]0, \infty[\rightarrow \mathbb{C} \setminus P_c$ with $R_\theta(t) = \varphi_c^{-1}(te^{2\pi i\theta})$.

$$c \text{ outside } \mathbb{M} \Rightarrow \mathcal{O}_{f_c}(0) \rightarrow \infty \Rightarrow c \text{ seen as } z \text{ outside } J_c \Rightarrow \varphi_c(c) \text{ is well-defined}$$

Let $\Phi(c) \equiv \varphi_c(c)$ then $\Phi: \mathbb{C} \setminus \mathbb{M} \rightarrow \mathbb{C} \setminus \mathbb{D}$ is an analytic isomorphism.

$\Phi(c)$ corresponds to external rays $R_\alpha:]1, \infty[\rightarrow \mathbb{C} \setminus \mathbb{M}$ with $R_\alpha(t) = \Phi^{-1}(te^{2\pi i\alpha})$.



The dynamics of f_c respects the levels and rays of $\Phi(c)$. Levels are mapped internally and rays are mapped to other rays. α represents not only the landing point but the entire ray and asymptotically the levels become circles and f_c behaves like $z \rightarrow z^2$ with $z = re^{2\pi i\alpha}$, $r \rightarrow r^2$ and $\alpha \rightarrow 2\alpha \pmod{1}$ and in binary form: $\alpha = \sum_{k=1}^{\infty} d_k 2^{-k} = 0.d_1d_2d_3 \dots$ with $d_i \in \{0,1\}$ maps to $0.d_2d_3d_4 \dots$ (left shift one step and chop).

Ex.
 $\frac{1}{3} \rightarrow \frac{2}{3} \rightarrow \frac{1}{3}$ or in binary form: $0.\overline{01} \rightarrow 0.\overline{10} \rightarrow 0.\overline{01}$ or in short form $\overline{01} \rightarrow \overline{10} \rightarrow \overline{01}$

$1/7 \rightarrow 2/7 \rightarrow 4/7 \rightarrow 1/7$ corresponds to $\overline{001} \rightarrow \overline{010} \rightarrow \overline{100} \rightarrow \overline{001}$ ($3/7 \leftrightarrow \overline{011}$ $5/7 \leftrightarrow \overline{101}$ $6/7 \leftrightarrow \overline{110}$)

Fractions in $[0,1]$ with finite decimal representation are periodic if $\alpha = 0 = 0.\overline{0}$ or $\alpha = 1 = 1.\overline{0} = 0.\overline{1}$ otherwise they are preperiodic, such as: $1/2 = 0.1 = 0.1\overline{0}$ and $7/8 = 101\overline{0}$.

Theorem:
 When p/q is in lowest form where p and q are relatively prime, $(p, q) = 1$ then:
 The binary decimal representation is periodic if q is even and preperiodic if q is odd.

Proof:
 p/q is preperiodic $\Leftrightarrow 2^A \alpha \equiv \alpha \pmod{1}$ for some $m \geq 1$.
 p/q is preperiodic $\Leftrightarrow 2^C \alpha \equiv 2^B \alpha \pmod{1}$ for some $C > B \geq 0$.

Let $p/q = p/(2^k r)$ with $(p, q) = 1$ and r odd
 Euler's theorem gives $2^{\phi(r)} \equiv 1 \pmod{r} \rightarrow 2^{\phi(r)} = jr + 1$ for some $j \in \mathbb{Z}$, $\phi(r)$ is Euler's totient function.
 $2^{(\phi(r)+k)} \alpha = 2^k \cdot 2^{\phi(r)} \alpha$
 $2^{(\phi(r)+k)} \alpha = 2^k (jr + 1) \alpha$
 $2^{(\phi(r)+k)} \alpha = 2^k \alpha + jp$
 $2^{(\phi(r)+k)} \alpha \equiv 2^k \alpha \pmod{1}$

$\phi(n)$ counts integers less than n that are relatively prime to n .

■

Theorem:

If $\alpha = p/q$ is in lowest term then the external ray of \mathbb{M} lands at a point c_α on the boundary of \mathbb{M} and:

- If q is odd then c_α is a root point of a bulb of M . (Periodic α on roots of bulbs around periodic points of \mathbb{M})
- If q is even then c_α is a Misiurewicz point. (Preperiodic α on preperiodic points of \mathbb{M})

Moreover when $p/q = 0.\overline{s_1 s_2 \dots s_n}$ is periodic then the root point where the p/q -ray lands separates a bulb of period n from a lower period bulb (with period dividing n) unless this root point is a cusp of a cardioid of one of the small copies of the Mandelbrot set in \mathbb{M} .

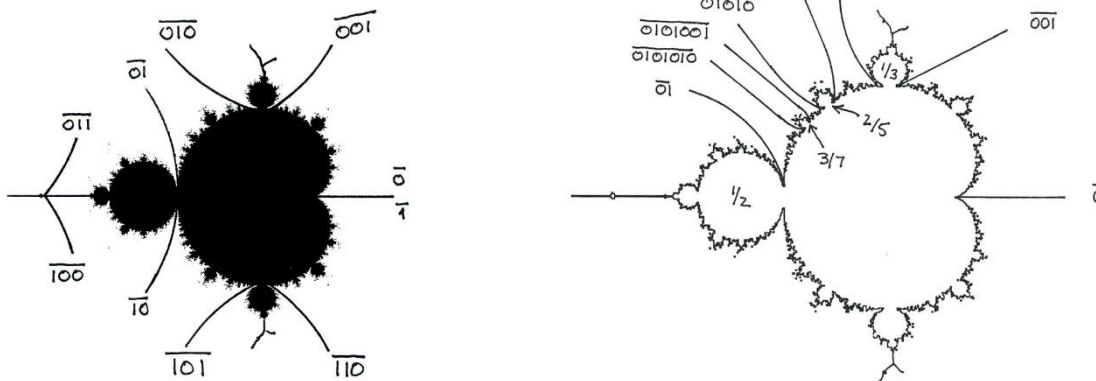
The proof of this theorem is long and messy. It can be read in the book *Complex Dynamics* by L. Carleson.

External angles of root points

External angles of rays that land at pinch points of p/q -bulbs attached to the main cardioid can be calculated by an algorithm called **Schleicher's algorithm**.

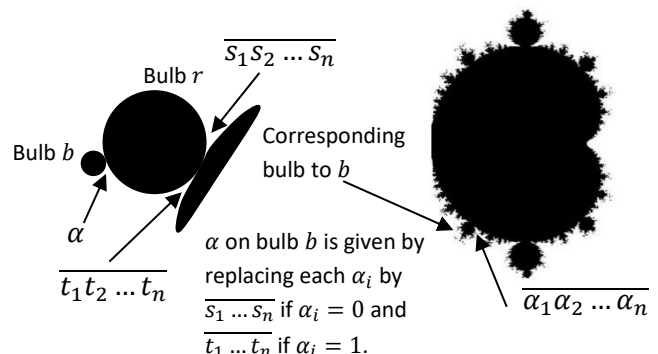
The ray that land at the cusp of the main cardioid is $\alpha = 0 = 1$. The upside of the ray is $0 = 0.\overline{0} \leftrightarrow \overline{0}$ and the bottom side is $1 = 0.\overline{1} \leftrightarrow \overline{1}$. For the $1/2$ -bulb with root at $c = -3/4$ and period 2 there are two possibilities for $0.\overline{s_1 s_2}$. They are $0.\overline{01} = 1/3$ and $0.\overline{10} = 2/3$. These rays are the initial conditions for the inductive Schleicher algorithm.

The biggest bulb between p_1/q_1 and p_2/q_2 is given by Farey addition $p_1/q_1 \oplus p_2/q_2 \equiv (p_1 + p_2)/(q_1 + q_2)$. The biggest cusp on the upper side between $0/1$ and $1/2$ is $1/3$ so the period is 3 and the rays have external angles of the form $0.\overline{s_1 s_2 s_3}$. To get the ray closest to the cusp start with the cusp angle $\overline{0}$ and concatenate the angle of the ray at bulb $1/2$ closest to the $1/3$ -bulb, $\overline{0} \boxplus \overline{01} = \overline{001}$. To get the ray at the other side of the pinch point add them in the opposite order, $\overline{01} \boxplus \overline{0} = \overline{010}$.



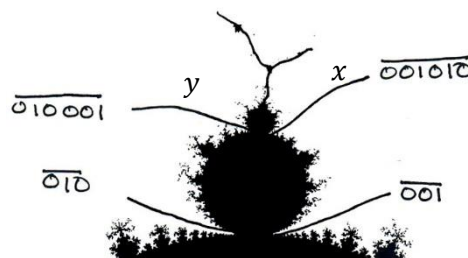
This procedure gives external angles for all rays at root points of the main cardioid. The lower period-3 bulb has external angles $\overline{10} \boxplus \overline{1} = \overline{101}$ and $\overline{1} \boxplus \overline{10} = \overline{110}$. Only two period-3 possibilities remain $\overline{011}$ and $\overline{100}$. These are the external angles of the cusp of the mini-Mandelbrot on the real axis whose cardioid has period 3. This can be compared to the period-3 window of the bifurcation diagram of the logistic map.

External angles of a bulb b attached to other bulbs than the main cardioid are given by another algorithm, the **tuning algorithm**. For bulb b assume a root bulb r with rays $\overline{s_1 \dots s_n}$ and $\overline{t_1 \dots t_n}$ at its root points. Bulbs are organized in the same manner along all bulbs so there is a corresponding bulb at the main cardioid.



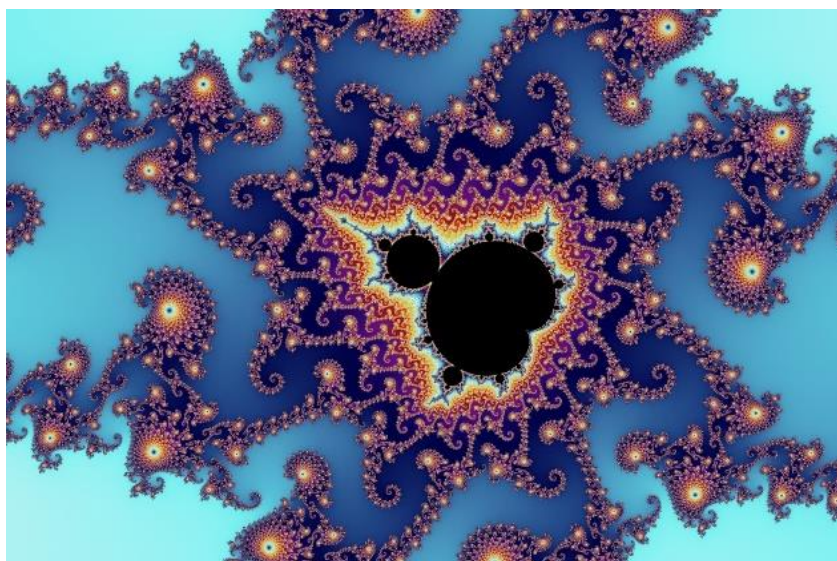
To get x start with $\overline{01}$ and replace 0 with 001 and 1 with 010, resulting in $x = \overline{001010}$.

To get y start with $\overline{10}$ and replace 0 with 001 and 1 with 010, resulting in $y = \overline{010001}$.



Schleicher's algorithm generates all rays attached to the main cardioid i.e. to all reference buds.

With knowledge of the root-rays and the tuning algorithm we can calculate angles for all bulbs attached to bulbs springing from the root bulb. The only external angles of roots that remain are the angles at the cusps of mini-Mandelbrots.



External angles of Misiurewicz points

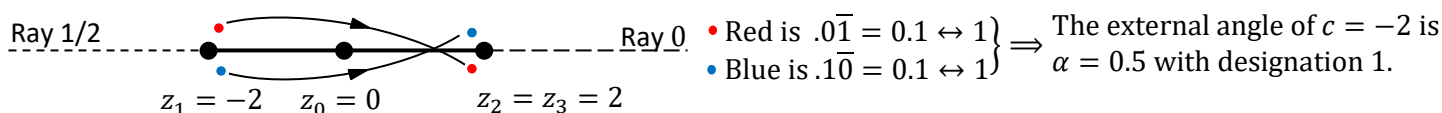
External angle of a rays landing on preperiodic points i.e. Misiurewicz points where $f_c^k(0) = f_c^{k+n}(0)$ can be calculated using the dynamics of the iteration by f_c on the corresponding Julia set and the asymptotic dynamics at the end of the rays, $z \rightarrow z^2$.

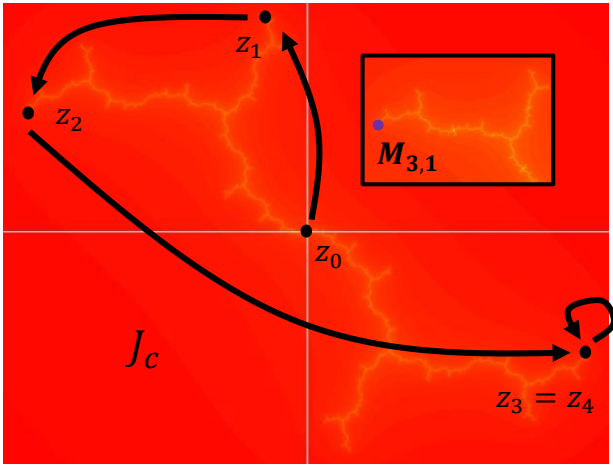
The procedure is an elaborate version of what you do when you want the binary representation of a real number $x \in [0,1[$. Apply $x \rightarrow x^2 \pmod{1}$ repeatedly and write 1 if the result is $\geq 1/2$ and 0 otherwise. To do this on a Julia set, strip J_c to its tree structure and follow the forward orbit $\mathcal{O}_{f_c}(0) : 0, c = f_c(0), f_c^2(0), \dots$ in the tree structure until you get into a loop. The tree structure is called a **Hubbard tree**. Join the external rays $\alpha = 0$ and $\alpha = 1/2$ to the tree and they will separate the plane into two parts, one counter-clockwise from ray 0 to ray 1/2 that represents being below $1/2$ and one part from ray 1/2 back to 0 that represents above $1/2$.

Start with two points at $z_1 = f_c(0)$, one above and one below the branch at z_1 and follow their iterations by f_c on the tree until you get into the loop. If $z_1 = c$ represents the end of a filament the two pathways should represent the same external angle.

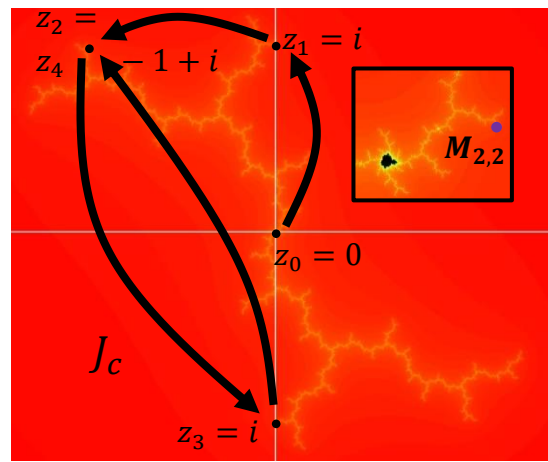
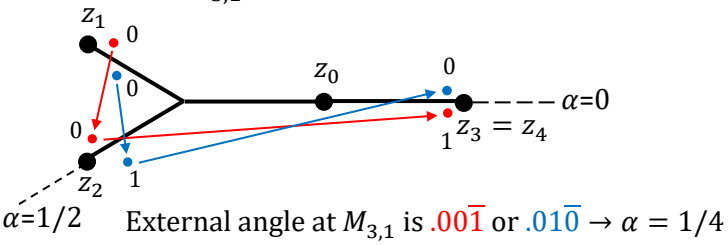
Ex.

$c = -2$ with $J_c = [-2,2]$ and $\mathcal{O}_{f_{-2}}(0) = 0, -2, 2, 2, \dots$

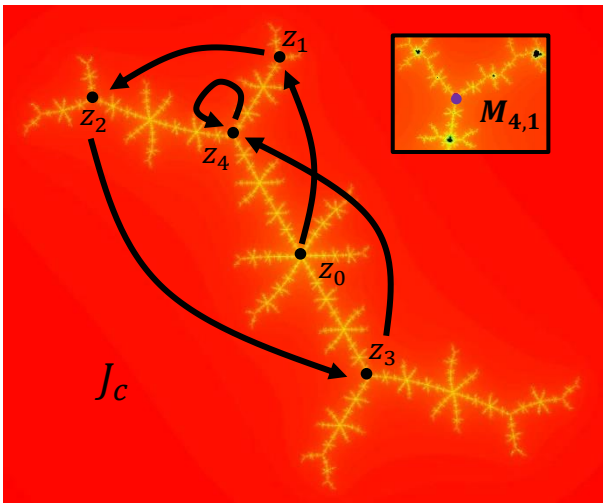
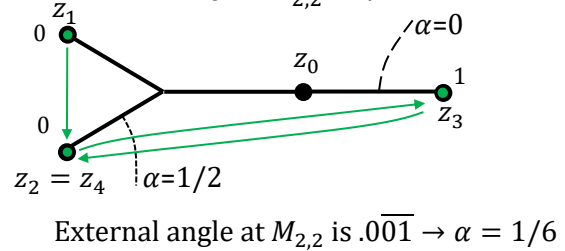




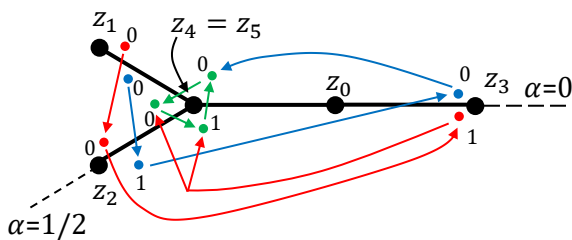
$$c = M_{3,1} = -0.22818 + 1.11514i$$



$$c = M_{2,2} = i$$



$$c = M_{4,1} = -0.10109 + 0.95628i$$

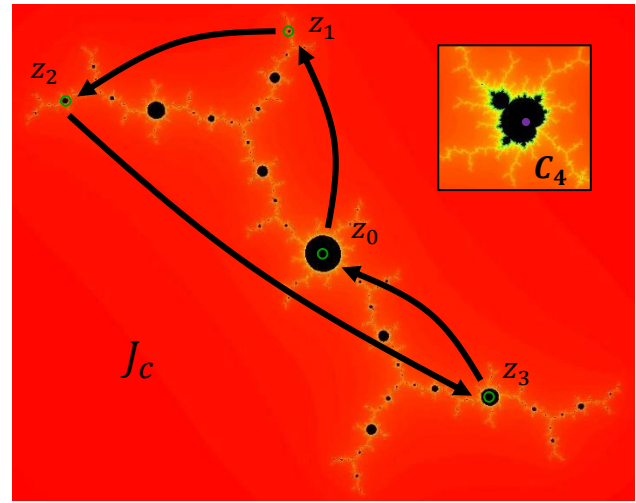


The Hubbard tree leads to three options:

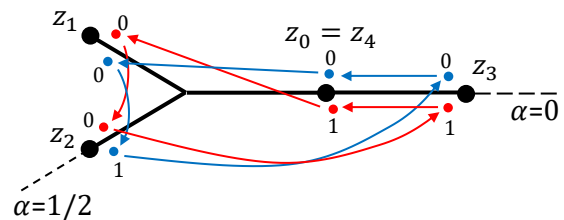
$$01000\bar{1} \leftrightarrow 15/56 \text{ and } 00101\bar{0} \leftrightarrow \alpha = 9/56$$

$$0011\bar{0} \leftrightarrow \alpha = 11/56$$

$M_{4,1}$ branches to 3 rays and 3 external angles



$$c = C_4 = -0.15652 + 1.03225i$$

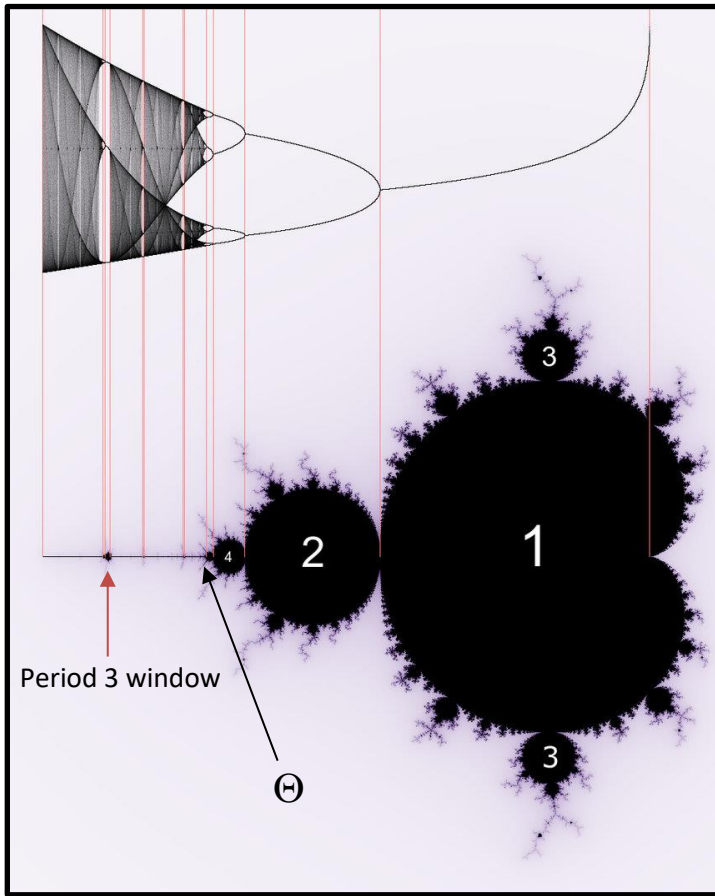


Hubbard trees for periodic points can be used to calculate external angles at the roots of the component they are centered in.

This example gives the external angles at the cusp of the period-4 cardioid of a mini-Mandelbrot.

$$001\bar{1} \leftrightarrow \alpha = 3/15 \text{ and } 010\bar{0} \leftrightarrow 4/15$$

The Mandelbrot set on the real axis and beyond



Bifurcations of the logistic map line up with pinch points in the Mandelbrot set. Each bulb corresponds to a specific period of the limiting cycle.

The number 3 for the biggest bulb in the complex direction indicates a limiting cycle of period 3 and a tri-furcation at the root between cardioid and bulb.

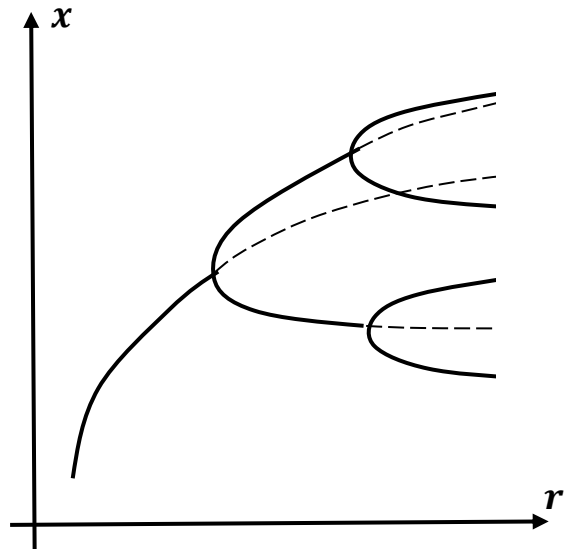
Going in the forward direction, to the biggest bulb for each component means a series of bifurcations.

The period doubling in the buds along the real axis is a direct parallel to the logistic map $x \rightarrow rx(1 - x)$ where bifurcations the interval lengths approach a geometric series that converge on an irrational number, r_∞ .

In the 1-dimensional setting of the logistic map there are pitchfork bifurcations where an attractive cycle of period 2^n split into an attractive cycle of period 2^{n+1} while the previous stable cycle turns unstable when the derivative passes the critical value $|Df_r^{2^n}(x_0)| = 1$, going from being attractive below one to repelling above one.

The difference when going from \mathbb{R} to \mathbb{C} is that we get buds from the main cardioid of period 1 to buds of any period n . In different direction there will be n -furcations of any $n > 1$.

Along the real axis there will only be bifurcations even though they may start from a cardioid of any period. The period-3 window corresponds to bifurcations 3,6,12,....



The Tuning algorithm can be used to get the external angles for rays that land on bifurcation points on the upper and lower sides of the real axis.

The upside external angles are: $\overline{01} \leftrightarrow 1/3$ $\overline{0110} \leftrightarrow 2/5$ $\overline{01101001} \leftrightarrow 7/17$ etc.

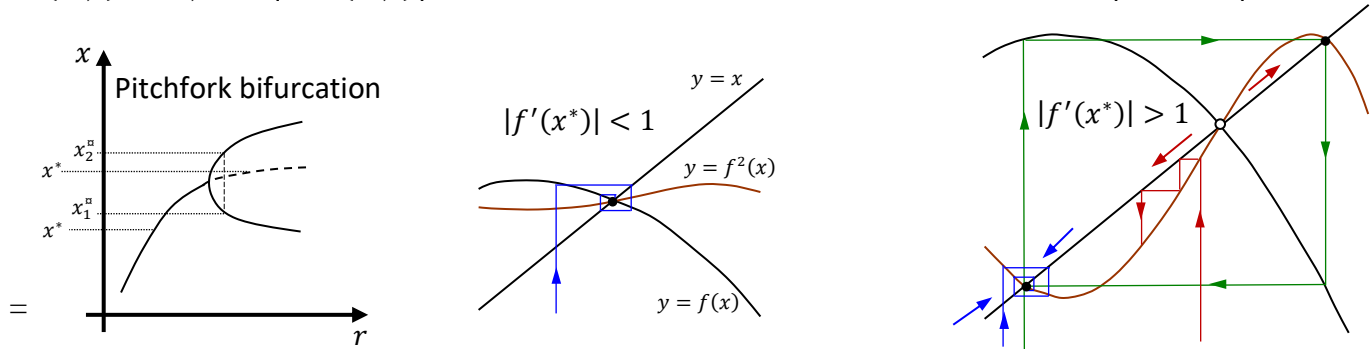
with irrational limit, the **Morse-Thue number**. The limiting point on \mathbb{R} is Θ , the **Feigenbaum-Myrberg point**.

Along the axis of each mini-Mandelbrot is a similar bifurcation sequence that converges to a limit point.

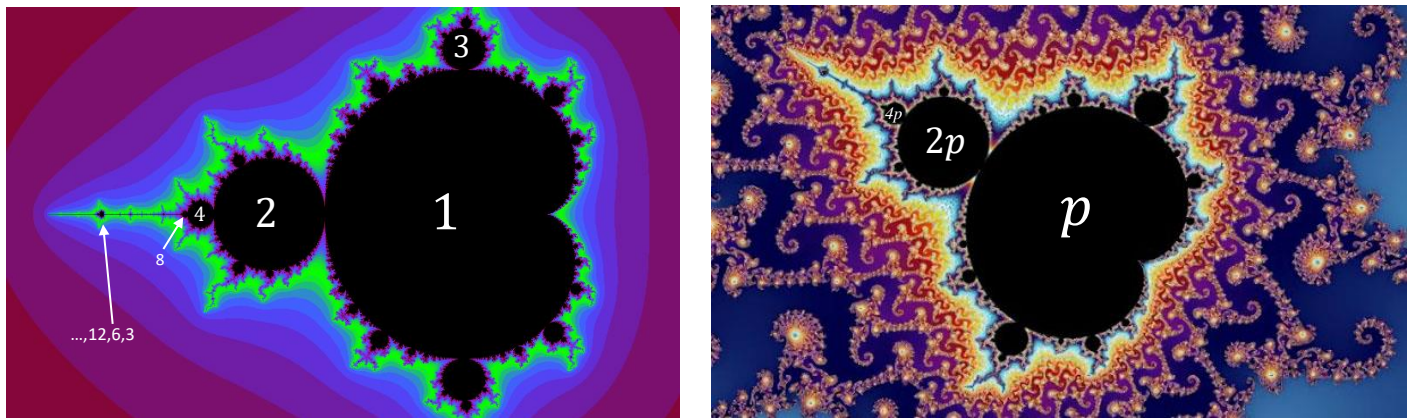
The mini-Mandelbrot that starts with period 3 on the real axis and a cusp at $c = -1.75$ has a similar series of upper and lower external angles with irrational limits.

The upper external angles are: $\overline{011} \leftrightarrow 3/7$ $\overline{011100} \leftrightarrow 4/9$ $\overline{011100100011} \leftrightarrow 29/65$ etc.

Bifurcations of the logistic map $f(x) = rx(1 - x)$ happens when attracting fixpoints of f , where $f(x^*) = x^*$ and $|f'(x^*)| < 1$ becomes repelling with $|f'(x^*)| > 1$ which gives rise to an attracting 2-cycle, with $f^2(x_{1,2}^n) = x_{1,2}^n$ and $|Df^2(x_{1,2}^n)| < 1$ and similarly for 2^n -cycles $\rightarrow 2^{n+1}$ -cycle when $|Df^{2^n}(x)| \geq 1$.



For $f_c(z) = z^2 + c$ similar bifurcations occur along the main axis of every Mandelbrot body:



Budding in other directions than along the main axis means going from an attractive cycle of period p to an attractive cycle of period $k \cdot p$ with $k = 3, 4, 5, \dots$. To see how this can happen, let's look at bulbs along the cardioid rim and especially the period-3 bulb in the upper halfplane of \mathbb{C} .

When the complex single attracting fixpoint in the cardioid body loses its attractive power:

$$\begin{cases} f_c(z) = z \\ |f'_c(z)| = 1 \end{cases} \rightarrow \begin{cases} z^2 + c = z \\ |z| = 1/2 \end{cases} \rightarrow z = \frac{1}{2}e^{i\omega} \rightarrow \frac{1}{4}e^{2i\omega} + c = \frac{1}{2}e^{i\omega} \rightarrow c = \frac{1}{4}(2e^{i\omega} - e^{2i\omega})$$

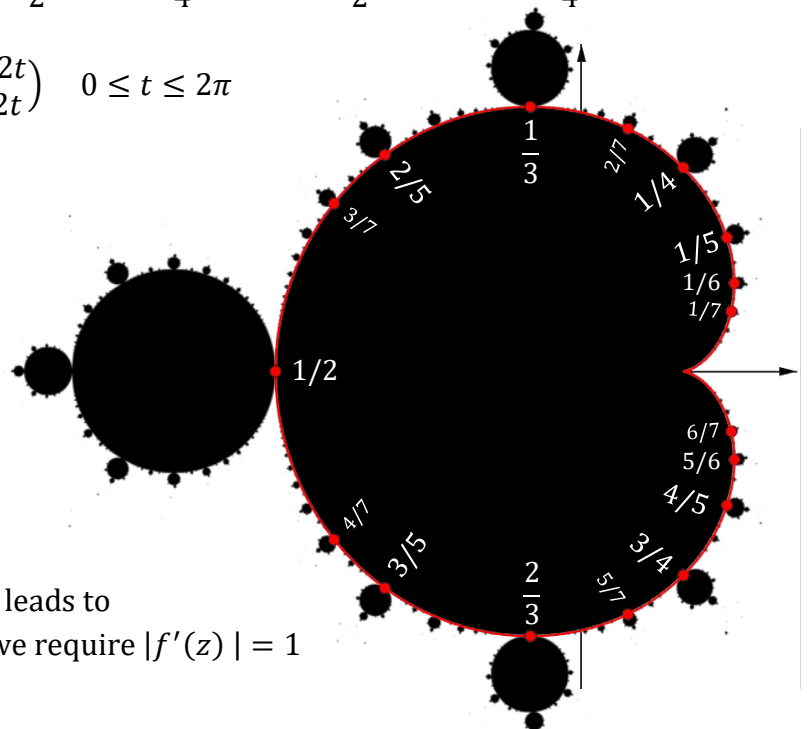
In parametric form: $\begin{pmatrix} x \\ y \end{pmatrix} = \frac{1}{4} \begin{pmatrix} 2 \cos t - \cos 2t \\ 2 \sin t - \sin 2t \end{pmatrix} \quad 0 \leq t \leq 2\pi$

which is the equation of a cardioid.

$$\begin{pmatrix} x \\ y \end{pmatrix} = \frac{1}{4} (2e^{2\pi i \cdot \alpha} - e^{4\pi i \cdot \alpha}) \quad 0 \leq \alpha < 1$$

To the right Mandelbrot set with cardioid on top with dots at p/q for $q = 2, 3, \dots, 7$. It appears that the p/q -bulb with period q and iteration jumping p petals each time corresponds to $\alpha = p/q$.

$\alpha = 1/2$ leads to a bulb at $c = -3/4$ which leads to $z^2 - 3/4 = z$ with solution $z^* = -1/2$ if we require $|f'(z)| = 1$



$f'(z^*) = -1$ for the $1/2$ bulb corresponds to two new fixpoints splitting of in two opposite directions along \mathbb{R} . In the complex plane \mathbb{C} the direction of $f'(z)$ is free and when $\arg f'(z) = 2\pi/q$ we might expect, not a bifurcation but a q -furqation. To investigate this idea, let $\alpha = 1/3$.

$$a = \frac{1}{3} \rightarrow c = \frac{1}{4}(2e^{2\pi i/3} - e^{4\pi i/3}) = \frac{-1 + 3\sqrt{3}i}{8} = -0.125 + i \cdot 0.649 \dots \quad \text{Root point of period 3 bulb.}$$

$$z \rightarrow z^2 + \frac{-1 + 3\sqrt{3}i}{8} \text{ with fixpoints decided by: } z^2 + \frac{-1 + 3\sqrt{3}i}{8} = z \rightarrow z^* = 1/2 \pm \sqrt{3/4}e^{-30^\circ \cdot i}$$

Requiring $|f'(z)| = 1$ as before gives $z^* = e^{120^\circ \cdot i}/2$ with $f'_c(z^*) = 2z^* \rightarrow f'_c(z^*) = e^{120^\circ \cdot i}$ which shows that the fix point splits in 3 directions, neither attracting nor repelling at the root point where $|f'_c(z)| = 1$ to start with but it then becomes attractive with $|f'_c(z^*)| < 1$ as c moves into the period-3 bulb.

To get an idea of what happens below and above, let's look at iterations on and around the prisoner sets for:

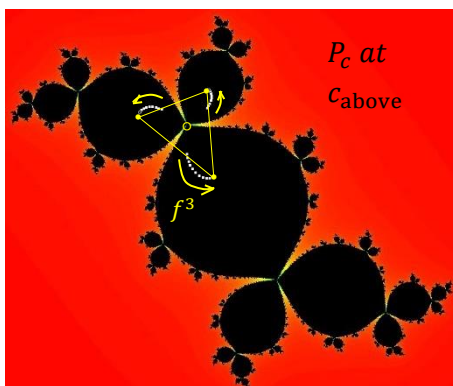
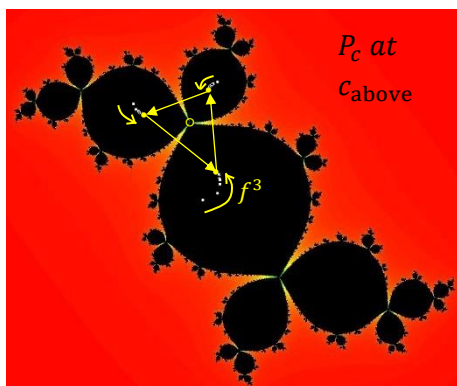
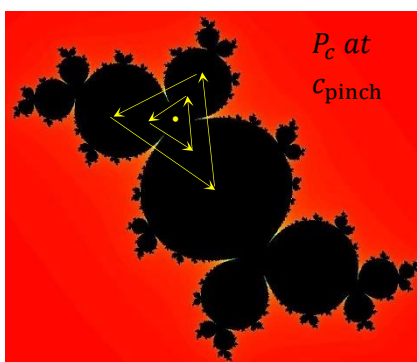
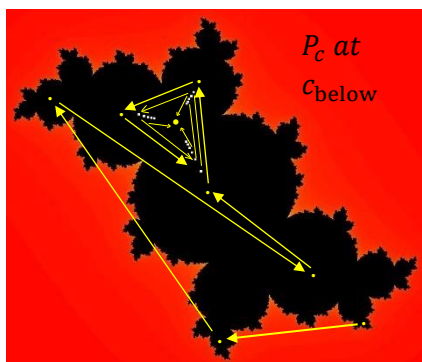
$$c_{\text{below}} = -0.125 + 0.62i \quad c_{\text{pinch}} = (-1 + 3\sqrt{3}i)/8 \quad c_{\text{above}} = 0.68$$

$$c = -0.125 + 0.62i \rightarrow \text{Relevant fixpoint of } f \quad z^* = -0.241 + 0.418i \text{ with } f'(z^*) = 0.965 \cdot e^{120.01^\circ \cdot i}$$

$$c = -0.125 + 0.68i \rightarrow \text{Attracting fixpnt of } f^3 \quad z^* = \begin{cases} -0.532 + 0.498i \\ -0.140 + 0.653i \\ -0.0899 + 0.151i \end{cases} \quad Df^3(z^*) = \begin{cases} 0.68e^{i \cdot (-0.22^\circ)} \\ 0.68e^{i \cdot (-0.22^\circ)} \\ 0.68e^{i \cdot (-0.22^\circ)} \end{cases}$$

$$\text{Repelling fixpoint of } f^3 \quad z^* = -0.259 + 0.448i \quad Df^3(z^*) = 1.10e^{0.028^\circ \cdot i}$$

$$\text{At } c = (-1 + 3\sqrt{3}i)/8 \quad z^2 + c = z \rightarrow z = \frac{1}{2} \pm \left(\frac{3}{4} - \frac{1}{2}i\right) \rightarrow z^* = \frac{e^{120^\circ \cdot i}}{2} = -0.25 + 0.433i \rightarrow f'(z^*) = 2z^* = e^{120^\circ \cdot i} \quad D(f^3(z^*)) = f'(z_1^*) \cdot f'(z_2^*) \cdot f'(z_3^*) = 1 \quad z^* \text{ is indifferent fixpoint}$$



The pictures show iterations at three values of c .

c_{below} in the period-1 cardioid with one attractive fixpoint.

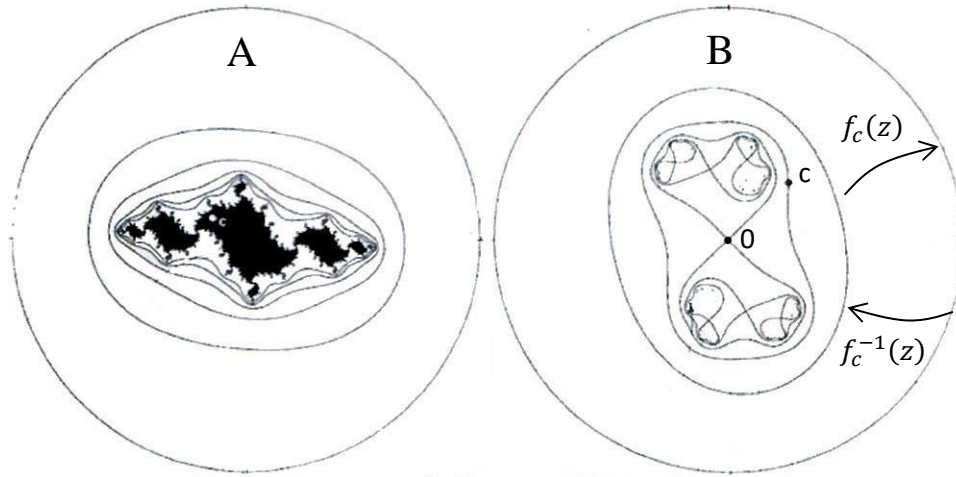
c_{pinch} at the root of the period-3 bulb with an indifferent fixpoint.

c_{above} in the period-3 bulb above the cardioid with attractive 3-cycle that attracts iterations from inside and outside the 3-cycle.

Iterating from the gorges between the petals leads to outward spirals, out from the valleys to infinity.

Further analysis of the Mandelbrot set

Time to round of the analysis of the Mandelbrot set with some final remarks. First a recap of the proof that \mathbb{M} , defined as the set of connected Julia sets can be seen as c for which $z_n \rightarrow \infty$ when $z_{n+1} = z_n^2 + c$ and $z_0 = 0$.



$f_c(z) = z^2 + c$ maps large circles into much larger circles. $z = \infty$ is a super-attracting fixed point with J_c as its basin of attraction. Start with a large circle far outside c and look at its inverse image $z_n = \pm\sqrt{z_{n+1} - c}$. Take successive inverse images of this initial large circle. As the radius goes down like $r_{n+1} \approx \sqrt{r_n}$ we will eventually approach c .

The inverse images of circles must be continuous closed curves that will eventually get into 1 of 3 cases

- A single simple closed curve. When z_{n+1} rotates around the bigger circle two points $\pm\sqrt{z_{n+1} - c}$ will rotate around the circle.
- Two separate orbits, each with one of the solutions $\pm\sqrt{z_{n+1} - c}$.
- A transitional figure formed like 8 or ∞ .

If all inverse images are simple closed curves, then the filled Julia set \mathbb{P}_c must be connected as seen in case A. If not then there will be a first 8 and a double root which means that $\pm\sqrt{z_{n+1} - c}$ has to be ± 0 i.e. $z_{n+1} = c$ and the figure 8 crossing occurs at $z = 0$ which then maps to $z = c$ as shown in case B.

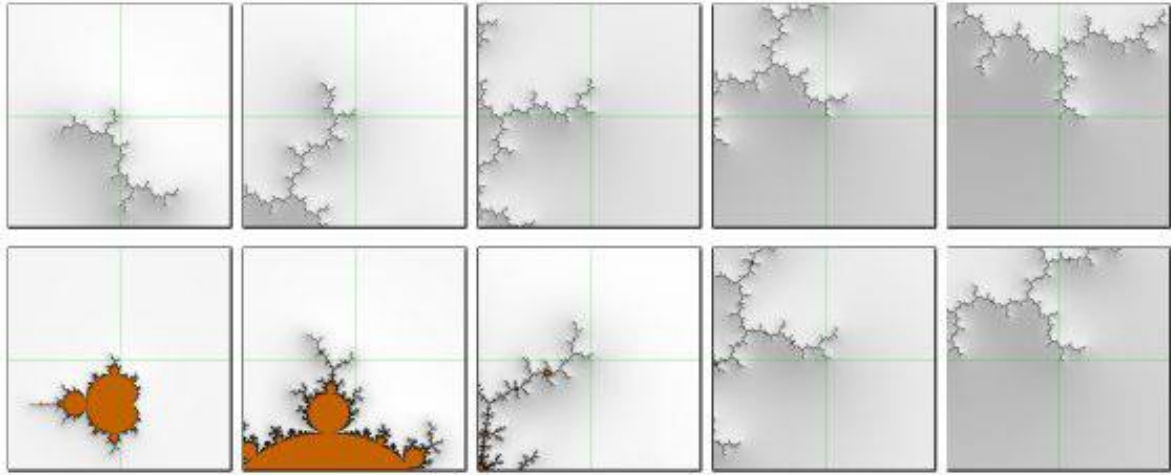
In case A we never reach c so it is inside \mathbb{P}_c and must stay confined when iterated. In the disconnected case $z = 0$ will iterate to ∞ .

\therefore Categorizing \mathbb{C} into parts with connected/disconnected Julia set, J_c can be decided by looking at whether the iterates of $z_0 = 0$ escape to infinity or not.

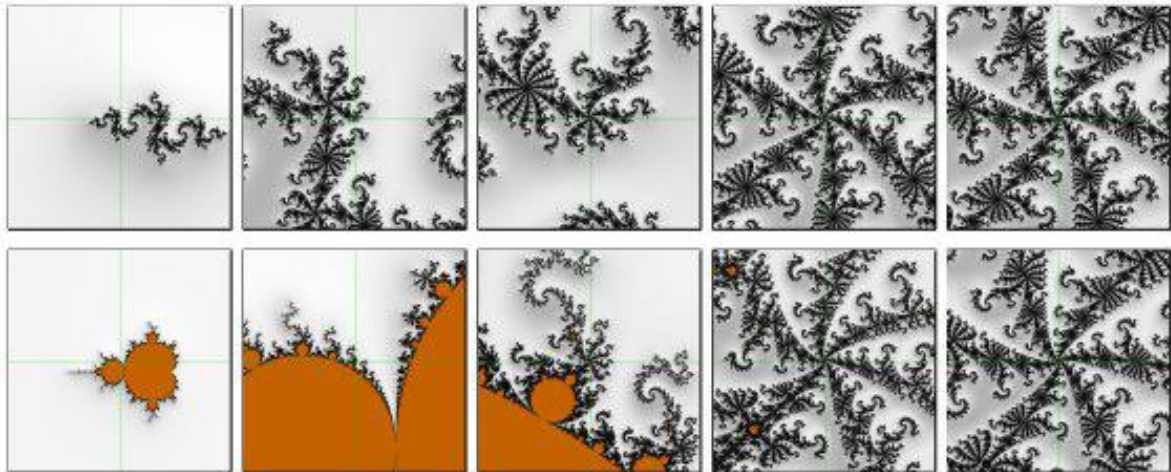
The border of the Mandelbrot set is a topological circle that can be parametrized by the external angle. What then is the Hausdorff dimension of this fractal boundary and does it vary between different parts of $\partial\mathbb{M}$?

The answer is that both connected Julia sets and the boundary of \mathbb{M} has dimension 2, $\dim_{\text{H}}(\partial\mathbb{M}) = 2$. The equality of $\dim_{\text{H}}(J_c)$ and $\dim_{\text{H}}(\partial\mathbb{M})$ is no coincidence, it is connected to the Tan Lei theorem on similarity between \mathbb{M} and J_c .

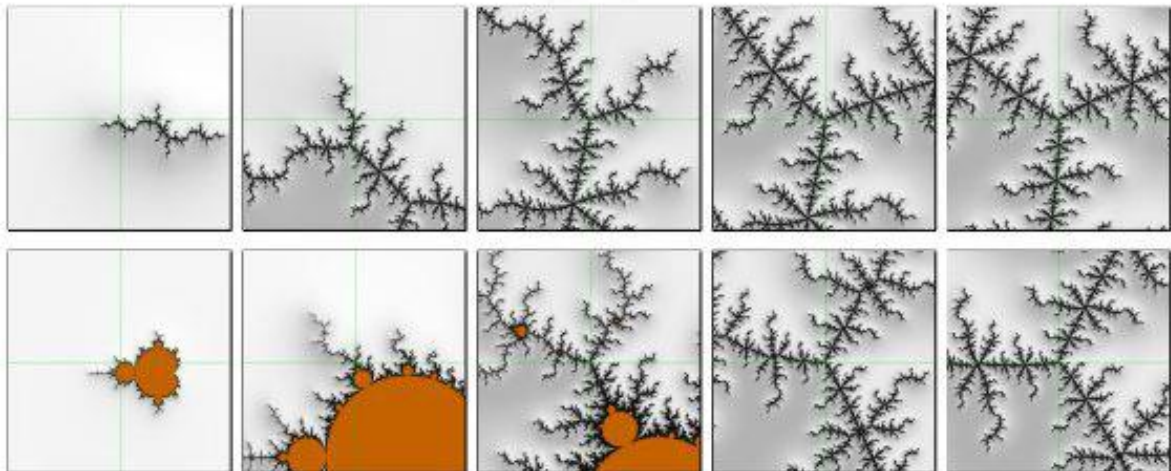
Zooming in on a Misiurewicz point, a point c whose critical orbit $z_0 = 0, z_1, z_2, \dots$ is preperiodic $z_k = z_{k+p}$ reveals another fascinating aspect about the Mandelbrot set.



J_c and \mathbb{M} around the point $c = i$



J_c and \mathbb{M} around the point $c = -0.8597 + 0.2348i$



J_c and \mathbb{M} around the point $c = -1.1623 + 0.2923i$

The more you zoom in on J_c and \mathbb{M} around c the more they resemble each other. This property is described in **Tan Lei's theorem**. If c is a Misiurewicz point then:

- J_c and \mathbb{M} are asymptotically self-similar in the point $z = c$ using the same multiplier $\rho = Df_c^p(z_k)$.
- The limit objects L_J and $L_{\mathbb{M}}$ differ only by a scaling and rotation factor $\lambda \in \mathbb{C}$.

Remember that Misiurewicz points are dense in $\partial\mathbb{M}$. The boundary of \mathbb{M} is like a table of contents for what different J_c look like.

There is another twist to this story. Close-ups of \mathbb{M} near $\partial\mathbb{M}$ always result in small copies of \mathbb{M} in every region and Tan Lei's theorem states that the similarity with J_c increases as we zoom but Julia sets can have no Mandelbrot copies in them since J_c has empty interior.

So how can J_c still be increasingly self-similar with \mathbb{M} that contains mini copies of itself all the way down. The explanation lies in how fast the mini- \mathbb{M} s decrease in size compared to the pace in increasing zoom-factor.

There are still things about the Mandelbrot set that are not known or haven't been proved yet.

To reconstruct the prisoner set \mathbb{P}_c from the disk model with external angles on the perimeter of a circle and where some external angles are pinched together you rely on J_c being locally connected. This follows from the **Caratheodory theorem**.

There are Julia sets that are connected but not locally connected and some that are connected but still not proven to be locally connected.

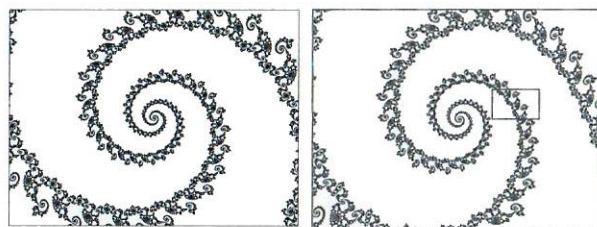
The reconstruction of \mathbb{M} from external angles and their pinchings depends on \mathbb{M} being locally connected. This has not been proven but is believed to be true.

Another open question is whether there are any **queer components**. If $f_c(z)$ has an attracting cycle then c is part of the interior of \mathbb{M} , not a part of $\partial\mathbb{M}$. Does the opposite apply? Does every point in the interior of \mathbb{M} correspond to an f_c with an attracting cycle? The bulbs we have described have attracting cycles. Could there be other types of components in \mathbb{M} ? The existence of these so-called queer components is an open question. If they exist it should be possible to spot them in a computer-generated image of some part of \mathbb{M} . The pinch disk model allows no queer components. If \mathbb{M} is locally connected there can be no queer components. The opposite is not true, local connectedness is a stronger statement. There is more that could be said about the analysis of the Mandelbrot set, such as **Yoccoz puzzles** and **laminations** but it's time to move on.

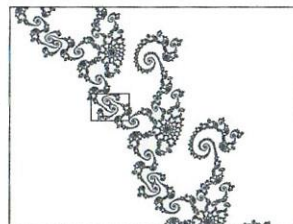
Mandelbrot sets in theory and applications

The Mandelbrot set is part of mathematics. It will pop up in applications of the physical world that relies on the same type of mathematical models. One such example is phase transitions and renormalization used to study magnetic domains and magnetization as the temperature drops below T_c where scale invariance occurs. The passage through $\partial\mathbb{M}$ is like a mathematical phase transition between different properties of J_c .

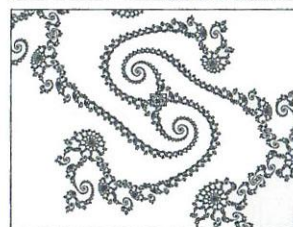
The Mandelbrot set is a general phenomenon of non-linearity. Other non-linear functions $f(c, z)$ have their own twisted versions of \mathbb{M} .



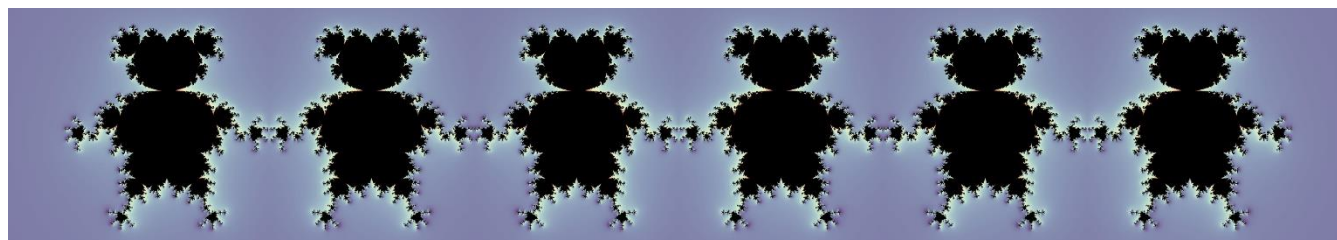
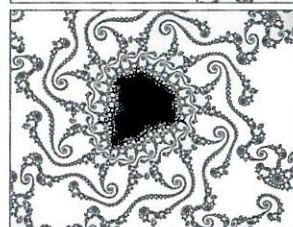
To the left is a zoomed image of J_c . To the right is \mathbb{M} , zooming in at $c = -0.77568377 + 0.13646737i$ same c as J_c to the left.



The left contains no mini-copies of \mathbb{M} but the right image contains an infinity of mini- \mathbb{M} s.



And still they look so similar in the beginning.



A series of Mandelbrot sets based on $f(c, z) = -icz^5 + 1$.